Published in final edited form as:
Compr Physiol. ; 2(1): 295–319. doi:10.1002/cphy.c100070.

Mechanics and Function of the Pulmonary Vasculature: Implications for Pulmonary Vascular Disease and Right Ventricular Function

Steven Lammers[1,2], **Devon Scott**[2], **Kendall Hunter**[2], **Wei Tan**[2], **Robin Shandas**[2], and **Kurt R. Stenmark**[*,1]

[1]Department of Cardiovascular Pulmonary Research, University of Colorado Denver, Aurora, Colorado

[2]Department of Bioengineering, University of Colorado Denver, Aurora, Colorado

Abstract

The relationship between cardiac function and the afterload against which the heart muscle must work to circulate blood throughout the pulmonary circulation is defined by a complex interaction between many coupled system parameters. These parameters range broadly and incorporate system effects originating primarily from three distinct locations: input power from the heart, hydraulic impedance from the large conduit pulmonary arteries, and hydraulic resistance from the more distal microcirculation. These organ systems are not independent, but rather, form a coupled system in which a change to any individual parameter affects all other system parameters. The result is a highly nonlinear system which requires not only detailed study of each specific component and the effect of disease on their specific function, but also requires study of the interconnected relationship between the microcirculation, the conduit arteries, and the heart in response to age and disease. Here, we investigate systems-level changes associated with pulmonary hypertensive disease progression in an effort to better understand this coupled relationship.

Introduction

The pulmonary and systemic circulatory systems are similar in that both circulate the same blood volume via a pulsatile fluid pump at the same periodicity (47). However, the pulmonary circulation is a system of low resistance, about one-sixth that of the systemic circulation (55, 103). Correspondingly, the pulmonary arterial pressure is approximately one-sixth that of the systemic, Figure 1. The right ventricle requires approximately one-fifth of the energy of the left ventricle to move the same amount of blood through the much lower resistance offered by the lung vasculature (48). The right ventricle is therefore a low-pressure high-volume pump which requires efficient ventricular-vascular coupling to move the total blood volume through the pulmonary circulation. Thus, and importantly, the material stiffness of large conduit vessels is lower in the pulmonary than systemic circulation and the hydraulic capacitance of the pulmonary circulation is quite significant (52). This large capacitance allows for the normal pulmonary circulation to accommodate a large range of blood flows with little increase in pulmonary arterial pressure (18). These properties have lead to the idea that the normal mammalian right ventricle is, to a large degree, functionally isolated from sites of significant impedance mismatching in the

[*]Correspondence to kurt.stenmark@ucdenver.edu.

pulmonary vasculature, indicating that the pulmonary vasculature and right ventricle have adapted in such a way as to reduce the mechanical load on the heart and conserve energy (117, 139, 158).

The vascular load imposed on the heart muscle as a result of both downstream hydraulic resistance hemodynamics and coupled vascular capacitance is an important determinant of ventricular function and overall cardiac health (61, 108). In fact, while several factors contribute to the vascular load imposed on the right heart by the pulmonary circulation, the vast majority of this load is the result of these two-coupled hydrodynamic loads, which in tandem, define the work performed by the heart to move blood through the pulmonary circulation with each cardiac cycle. The first of these loads is the one associated with the downstream hydraulic resistance imposed by the arterioles and capillaries of the lung. In the pulmonary circulation, this resistive load is typically characterized by the measure of pulmonary vascular resistance (PVR), where PVR is defined as the ratio of the drop in mean pulmonary artery pressure (mPAP) across the pulmonary circuit, to cardiac output. The second of these loads is associated with the hydraulic capacitance provided by the elasticity of the conduit arteries during the cardiac cycle. Despite the fact that large vessels are critical in the coupling of the RV to the distal pulmonary circulation, there has been relatively little research directed specifically at the pulsatile hemodynamic alterations within the proximal pulmonary arteries (PA), which occur in the setting of pulmonary hypertension (PH). By focusing on these two hydraulic loads specifically, right ventricular (RV) afterload can be associated with both steady-state resistance, categorized by PVR, and dynamic compliance, defined by the pulmonary vascular stiffness (PVS) of the conduit PA (17, 19, 87, 88, 102, 115–117).

Most studies of PH focus heavily on PVR, which quantifies mean hemodynamic parameters of flow and pressure. Elevations in PVR have long been considered to be a defining attribute of PH (3, 6), given that increases in PVR are primarily responsible for increases in mPAP due to distal vasoconstriction, inward vascular remodeling (secondary to cell hyperplasia, hypertrophy, and matrix protein accumulation), inflammation, and thrombosis (95, 142, 143). These pathologies all change distal vascular diameter and/or overall flow area of the distal pulmonary circulation, and thus strongly affect resistance. This focus on relating PVR and PH is reasonable given that, clinically, the clearest hemodynamic manifestation of the disease is an increase in mPAP. Diagnostic and treatment paradigms have therefore focused on PVR and its reactivity to vasodilator therapy. The net result has been significant, but inadequate progress in the reduction of patient morbidity and mortality resulting from PH and right heart failure remains unsatisfactory (3, 6, 38, 39, 77). There are many potential explanations for this lack of overall success. Among them is the fact that as noted, distal resistance vessel evaluation neglects the functional importance of proximal vessels in maintaining RV pumping efficiency, and marked stiffening of the proximal vessels as happens with PH decreases this efficiency dramatically. Further, PVR measurement does not include the oscillatory component of hemodynamics, which has been shown to account for 30% to 40% of total hydraulic power requirements in healthy pulmonary circulation (87, 88).

The oscillatory components of pulmonary circulation encompass the hemodynamic variables of compliance, elasticity, wave velocity, and wave reflection. These oscillatory components can be characterized by the impedance of the pulmonary circulation, a hydraulic parameter, which defines the relationship between pressure and flow for a pulsatile fluid system (10, 19, 106, 129). To this end, the oscillatory component of pulmonary blood flow has been shown to be important in determining how the right ventricle is coupled to the lung vasculature (19, 115, 158, 159). Vascular oscillatory function is primarily dependent upon vessel geometry and the mechanical properties of the conduit artery vessel wall. Of

particular importance are the changes in stiffness of the proximal elastic arteries a finding, which has long been recognized as being intrinsic to PH (30, 44, 102) and as a determinant of flow propagation and pulsatility. Alterations in large artery stiffness have been shown to change the manner in which oscillatory energy is dissipated within the lung vasculature and suggest that increased PVS leads to enhanced transmission of oscillatory energy to the resistance region of the lung, a result which may lead to a feedback mechanism of PH disease progression (17, 72).Additional evidence suggests that changes in vessel stiffness of the pulmonary circulation may have an even larger impact on coupled cardiopulmonary hemodynamic function than do similar changes in systemic arterial stiffness (102, 158, 159).

Overall, unfortunately, the contribution of vascular stiffening to the derangement of pulmonary vascular function has not been well studied, and has been mostly neglected in both basic science and clinical studies regarding PH. The primary reasons for this appear to have been the lack of direct clinical data documenting the relationship between clinical outcomes and PVS diagnostics, and the difficulties in measuring PVS within the routine clinical evaluation of PH. This is beginning to change. Recent clinical work has highlighted the importance of PVS in the progression of PH (17, 19, 40, 56, 78, 150); mechanical studies have begun to elucidate the gross vascular changes responsible for stiffening; and existing and novel studies of cellular mechanotransduction suggest PVS may play a role in pulmonary disease pathogenesis (72, 73). Many of these concepts have been adopted by investigators studying the systemic vasculature in health and disease (9, 61, 91, 92, 106, 107, 124). Here, we propose that proximal vascular stiffening constitutes an important aspect of hypertensive disease progression within the pulmonary vasculature, and that disease progression can only be fully understood through a comprehensive evaluation of right heart (dys)function, changes in pulmonary artery oscillatory hemodynamics and structural and functional changes within the microvasculature of the lung.

Large and Small Vessel Function in Health and Disease

From a pathologic and functional perspective, there are two main categories of PA, elastic and muscular (Fig. 2). Large PA are of the elastic type, are located proximal to the heart, and serve both as a conduit for total pulmonary blood volume and as a hydrodynamic capacitor through artery compliance. The primary resistive structures in the pulmonary vasculature are the pulmonary arterioles; small muscular arteries whose function is to regulate the hydraulic resistance through vasoreactive changes in interluminal diameter and the capillary network of the lung, Figure 2. PVR measurement has been the standard diagnostic for evaluating the significance of constrictive and remodeling changes in the distal vasculature and the extent of vascular response to therapies. However, PVR is an inherently limited diagnostic in that it ignores PVS, an especially important omission given the inherently pulsatile nature of cardiac function and the importance of robust ventriculo-vascular coupling in maintaining hemodynamic efficiency through the pulmonary vasculature.

Hydrodynamic capacitance allows the conduit arteries to act as a pressure reservoir and to reduce flow pulsations from the cyclic action of the heart, which reduces the ventricular workload during systole and conserves energy expenditure for the heart by alleviating pulsatile stress and by dissipating wave reflections. Hydrodynamic capacitance of the PA, obtained through pulmonary vascular input impedance, has been shown to be a better predictor of clinical outcome in PH than that of PVR alone (40, 56, 78, 121). In fact, many studies of vascular function in systemic hypertension are documenting the substantial role played by the elastic proximal arteries in maintaining systemic vascular hemodynamic efficiency and reducing cardiac workload. Several investigators have shown the significant mechanical advantages conveyed by the elasticity of systemic conduit arteries in reducing overall hydraulic impedance and cardiac workload (10, 61, 102, 103, 105). Others have

correlated proximal artery stiffness and reduced compliance with cardiovascular mortality for patients with systemic hypertension. Elastic compliance of the conduit arteries also prevents the arterial pressure from rapidly decreasing at the heart valve after systole is complete and reduces the pulse wave velocity (PWV) and the after-load on the heart. It therefore stands to reason that PVS is an important and integral component of PH disease progression and resultant RV afterload elevation.

As the arterial lumen diameter decreases longitudinally along the pulmonary arterial bed, vascular morphology changes from elastic to muscular. As distance increases from the heart, the elastic lamina become less predominant, arterial elasticity decreases, and the smooth muscle cell layer begins to constitute the majority of the vessel wall thickness. Persistent distal vasoconstriction has been long noted as a feature of patients with pulmonary arterial hypertension (PAH) (59, 133, 134, 145), and likely is due to alterations in vasoactive mediator release from stressed/injured endothelial cells (12). Vascular reactivity to vasodilators such as inhaled nitric oxide, determined by acute reduction in PVR, remains an important part of clinical diagnosis (3, 4). Hypoxic animal models of PH all display persistent distal vasoconstriction (79, 96, 120, 132) that can be acutely reduced by vasodilators although this constriction appears to become less important in the more advanced disease state (34, 119, 132, 133) With time vascular remodeling and rarefaction contribute more significantly to the increases in resistance observed and are less responsive to traditional vasodilator therapy. Because small muscular arteries contribute most significantly to the overall cross-sectional area of the vasculature, reduction in luminal area or number of these vessels plays a significant role in determining the work required of the ventricle for propelling blood through the lung.

Vascular impedance

Pulmonary pressure and flow waveforms, while periodic, do not take the form of a simple sinusoid. However, Fourier transforms allow for any periodic signal to be represented by a series of sinusoidal waves of various frequencies, amplitudes, and phase angles. Therefore, the pulmonary pressure and flow signals can be represented using the following summation of cosine functions:

$$P(t)=\bar{P}+\sum_{n=1}^{n_{\max}} P_n \cos(n\omega_1 t-\alpha_n) \quad (1)$$

$$Q(t)=\bar{Q}+\sum_{n=1}^{n_{\max}} Q_n \cos(n\omega_1 t-C_n) \quad (2)$$

where $\bar{P}$ and $\bar{Q}$ are the mean pulmonary pressure and flow, t is the time, and α_n and C_n are the phase angles of the pressure and flow waves, respectively, and P_n and Q_n are the moduli of the pressure and flow waves. The fundamental frequency (f_1) is the inverse of the heart rate period, and ω_1 is the angular frequency in radians ($\omega_1 = 2\pi f_1$). The variable n is an integer value representing successive harmonic numbers, and for each value of n there is a sinusoidal wave with a specific frequency, amplitude (modulus) and phase angle.

Trigonometric forms are often difficult to work with and Fourier series are often represented as complex numbers. Using this approach, the different harmonics comprising the summation in the Fourier series can be represented as:

$$\dot{P}_n=P_n \exp[j(n\omega_1 t-\alpha_n)] \quad (3)$$

$$\dot{Q}_n = Q_n \exp[\, j(n\omega_1 t - C_n)] \quad (4)$$

where $j = \sqrt{-1}$. The input impedance can then be defined as:

$$Z(n) = \frac{\dot{P}_n}{\dot{Q}_n} \exp(C_n - \alpha_n). \quad (5)$$

At each harmonic, the input impedance is characterized by amodulus ($Z_n = \dot{P}_n/\dot{Q}_n$) and a phase angle ($\varphi_n = C_n - \alpha_n$). The impedance modulus is a measure of the relationship between pressure and flow of an oscillatory system in the same manner as resistance expresses this relationship under steady flow conditions. The impedance phase angle expresses the relationship between the phase of the pressure and flow waves, with a positive φ_n representing fluid flow leading pressure and a negative value indicating pressure leading flow within the artery. Equation 5 describes the impedance modulus at each frequency, including the zero harmonic (i.e., steady flow); what is buried in the formulation, however, is the idea that the harmonics are independent. In practice, this means impedance independently quantifies both the resistive (steady) and stiffness (pulsatile) loads faced by the heart, and was shown experimentally by Weinberg (150). By decomposing the pressure and flow waves into their constituent sinusoidal components the pressure and flow waves measured in the pulmonary circulation can be analyzed directly, and *in vivo* vascular resistance and stiffness can be measured. An example of pulmonary impedance modulus measurements within healthy and hypertensive patients is shown in Figure 3.

Hydraulic resistance to the steady, nonpulsatile, component of blood flow within the circulation is equal to the zero harmonic (Z_0), and is clearly elevated during PH, Figure 3. How the stiffness load is described has varied, with some groups choosing the characteristic impedance (Z_c) or first minimum of impedance (36, 76, 81, 85, 102, 114) and others using the magnitudes of the first several moduli (56, 150); however, all measures show elevated stiffness within PH circulation, Figure 3. (Z_c) is the input impedance in the absence of wave reflection and is typically determined experimentally by averaging the harmonics of a measured impedance curve from the first minimum up to the 8th or 10th harmonic (17, 105, 116). Determination of (Z_c) also allows for the theoretical separation of forward-traveling and backward-traveling waves and is useful in the analysis of reflected waves. While (Z_c) can offer insight into vascular mechanics, it also depends on vascular diameter; thus vascular geometry must also be considered when interpreting its values.

While impedance is clearly a better measure of total heart afterload compared to resistance alone, it has not been incorporated into standard clinical workflows. This is primarily because both pressure-time and flow-time histories are required, and such measurements are typically invasive. While pressure measurement is straightforward, flow has been measured with a highly invasive cuff-type flow meter (88) or flow catheter (49, 65, 138, 140) and more recently has been estimated with pulse-wave Doppler ultrasound (54). This last method holds greater promise for clinical application, in that such measurements have been shown to better predict one-year soft outcomes in pediatric pulmonary arterial hypertension (56). The reason for this improvement is clear: impedance describes both resistive and stiffness components of afterload, and thus is a better measure of afterload compared to PVR alone.

Changes in Pulse Wave Velocity, Waveforms, and Reflections with Pulmonary Vascular Stiffening

Proximal vascular stiffening and pulse wave velocity and wave reflections

Because the pulmonary arterial system consists of many branching tubes of varying diameter, and due to the nonuniformity of vessel wall stiffness throughout differing regions of the vasculature, the effect of wave reflections on the dynamics of the system must be considered. Stated simply, wave reflections occur in pulsatile fluid flow whenever there is a change in the characteristic impedance or geometry (i.e., branch point) of an arterial segment. Most often these changes in characteristic impedance are due to a discontinuity in vessel diameter or arterial wall stiffness, or as a result of arterial branching. When a pressure wave encounters one of these discontinuities, part of the energy of the pressure wave is redirected in the opposite direction of the incident, or forward moving, wave.

Cardiac pressure waves travel as a pulse with a finite linear velocity due primarily to the distensible nature of the vessel wall. PWV can be defined by the Moens-Korteweg relationship as:

$$\mathrm{PWV} = \sqrt{\frac{Eh}{\rho D}} \quad (6)$$

where E is the wall elastic modulus, h is the wall thickness, ρ is the blood density, and D is the vessel diameter. For pulsatile fluid flow within a segment of pipe, the velocity at which a pressure wave travels is dependent on the stiffness of the pipe wall, where stiffness is equal to the product of the elastic modulus and wall thickness (Eh) (11). If the wall of the tube is infinitely stiff and the fluid is assumed to be incompressible, as would be approximated by pulsatile flow of water in a length of steel pipe, the PWV is infinite and any change in the input conditions would be instantaneously translated to all locations along the length of the pipe. If, however, the tube wall is able to deform under the pulse pressure, then the velocity of the propagating wave front is finite and changes in inlet conditions are translated, over time, along the length of the tube. Typical aortic PWV values for healthy 20-year-old people average 8 m/s and increase linearly to 13.5 m/s by age 80 (2). Recent studies have illustrated the value of tracking changes in aortic PWV as opposed to mean blood pressure (MBP), over time, and the response to therapy with regard to patient outcome (29). Patients with elevated MBP, in whom PWV was also assessed, were initially treated with targeted weight adjustment and additional angiotensin-converting enzyme inhibitor, calcium antagonists or β-blocker therapy and were followed for more than four years. MBP and PWV were assessed in patients who lived and who died over the course of the study. Of the 59 patients who died, it was observed that aortic PWV began at a higher average value and rose, rather than fell, despite significant reduction in MBP resulting from antihypertensive treatment. These observations support the idea that aortic PWV, not blood pressure *per se* was a better indicator of hypertensive disease progression and death during the period of observation, Figure 4 (29).

In the systemic circulation, the PWV is such that the round-trip time needed for a pressure wave to propagate from the heart to the major peripheral reflection sites and back is such that, in many cases, the reflected pressure wave returns to the heart during systolic ventricular ejection and augments the pressure against which the heart must pump. This interaction between the incident and reflecting pressure waves is quantified by the augmentation index, which is a measure of the change in peak systolic pressure resulting from the reflected wave's interaction with the incident pulse pressure wave. In young adults, below the age of 20 years, the value of the augmentation index is typically less than zero and

the reflected wave interacts with the incident pulse during diastole. By the age of 30 the augmentation index occurs earlier, typically during late systole, while the augmentation index value remains less than or equal to zero. By middle age, the augmentation index becomes positive, with typical values around 20% (97, 103). This positive augmentation index indicates that the heart must pump blood against a pressure elevated by the reflected wave, which concurrently returns earlier in the pulse, typically during early systole and extending throughout the remainder of ventricular ejection. As arteries continue to stiffen either due to increased age or due to a disease such as hypertension, the augmentation index value continues to increase, up to 60% in many cases (97, 103), and the reflected wave returns earlier during systole, further elevating ventricular afterload by augmenting the incident pulse pressure at the aortic root during ventricular ejection (103).

Systemic augmentation index is dependent on aortic PWV, which is strongly correlated with patient mortality (9, 151). In turn, the PWV is dependent on fluid density, vessel diameter, and stiffness. Changes in blood density are typically very small in relation to the other dependent parameters therefore this variable does not strongly influence PWV. However, PWV is strongly dependent on both the vessel diameter and stiffness. Further, the *in vivo* operating diameter of the conduit arteries is dependent on both the vessel stiffness and the imposed hydraulic pressure load. Hydraulic pressure load is also somewhat a function of vessel stiffness due to the hydraulic capacitance component of the impedance of the circulatory system. Therefore, both the PWV and the augmentation index are strong functions of conduit vessel stiffness (11, 87). This dependence complicates assigning causal reasons for the correlation between elevated PWV and patient mortality. In other words, is the increased correlation between elevated PWV and patient mortality due to the change in hydrodynamics resulting from reflected waves and augmentation index specifically or are these symptomatic of increased vessel stiffness which is the real cause for increased cardiac workload? Given the complexity of the circulatory system, the answer to this question is not yet fully understood and more complex models of cardiovascular dynamics are ultimately needed to investigate these coupled effects.

Less is understood regarding reflected waves and their effects in the pulmonary circulation. Part of this discrepancy may result from the lack of significant change in measured augmentation index resulting from idiopathic PH, which averages an augmentation index value of 9% a value that is statistically equal to the control index value of approximately 10% (13, 112). However, secondary causes of PH and right heart dysfunction have been shown to have a significant impact on the value of the augmentation index and thus reflected waves. Zuckerman et al. documented reflected waves in calves with hypoxia-induced PH (158). They showed that while the normal pulmonary circulation has few wave reflections, changes in the viscoelasticity of the vessel wall can increase wave reflections. When pulmonary artery compliance is decreased and PWV is increased, reflected waves are returned to the pulmonary artery during systole rather then diastole, increasing the pulse pressure (13). In chronic pulmonary thromboembolism (CPTE) the augmentation index increases to approximately 26% (13, 100), which has been attributed to the pressure wave encountering the CPTE blockage and experiencing a large wave reflection. In scleroderma patients, the augmentation index is elevated in patients with both normal and hypertensive pulmonary pressures showing increases of 24% ± 18.9% and 20 ± 19.1% in control and PH scleroderma patients, respectively (112).

Effect of pulmonary vascular stiffness on pulse waveform—Elevated stiffness of the large capacitive arteries affects both the level of hydrodynamic capacitance of the system as well as the velocity and waveform of the pulsatile flow delivered to the more distal vasculature (158). While it is fairly obvious that stiffer arteries will deform to a lesser extent than more compliant vessels for the same pressure differential, it is less obvious how

changes in vascular wall properties affect both the flow and pressure waveforms of the cardiac pulse. Detailed explanations of the theoretically and experimentally derived oscillatory flows in both rigid and flexible tubes have been thoroughly discussed elsewhere (86, 88), and will not be presented here in detail. However, the effect of vascular stiffness on pulse flow dampening will be examined.

Interactions between large and small arteries relate the transmission of pulsatile pressure and flow through the pulmonary circulation. Large PA dampen flow pulsations resulting from intermittent ventricular ejection; consequently, small arteries deliver a semisteady optimal blood flow to the gas-exchange units of the lungs. Interactions between the macro-and microcirculations are based on pulse pressure and pulsatile flow waves (107, 122, 126). When the vessel walls of the large arteries stiffen, the compliance of the vascular system is reduced, and thus the capacity of these vessels to modulate flow pulsatility is diminished. Vascular remodeling leads to reductions in compliance of the system, which then requires a greater distending pulse pressure for a given change in artery cross-sectional area (104). This macrocirculation compliance thus regulates pulse pressures waves and influences the extension of pulsations into the microcirculation (122, 126).

The elevated downstream pulsatility due to increased vessel stiffness also causes both the tensile and shear stresses imposed on the endothelium to rise. Tensile stress is the result of blood pressure producing strains exerted perpendicular to the vessel wall, that is, the stress, which causes the vessel to distend in response to increased pressure load. Shear stress is the tangential frictional force imposed on the vessel wall (122) caused by rapidly moving blood flowing past an essentially stationary vessel lumen. A result of the decrease in arterial compliance is a concomitant increase in both forward blood velocity and shear stress on the arterial wall (74). Further, the increased distal pulse pressure causes tensile stresses to increase in proportion to the increase in pulse pressure (8). Therefore, the kinetic energy associated with cardiac ejection is transmitted further downstream and higher pulsatile flow, shear and tangential stresses are experienced by the smaller PA. Given that these distal arteries are unaccustomed to the hydrodynamics of this large pulse flow, distal arterial cells including endothelial, smooth muscle, and fibroblasts respond to the high-stress environment in a variety of ways, many of which exacerbate the distal vascular dysfunction associated with PH (73, 132). Further, increased vascular resistance in the microcirculation influences the pulse pressure in the macrocirculation where a higher pressure is required to advance blood flow when microcirculatory resistance is increased (35).

Stiffening of arteries alters the way that the pulmonary vascular system can respond to stress and pressure changes. When the buffering function of the vasculature decreases, pulsations from the heart are not efficiently dampened; this then alters the smooth near-continuous flow that normally dominates in downstream arteries (94). Therefore, arterial stiffening can increase pulsatile flow in the downstream arteries, which may lead to further microvascular damage (70); studies have shown that microvascular changes are closely related to the stiffness of large arteries (91, 107, 122, 126). Elevated pressures decrease the distensibilty of vascular walls, this change influences the pressure and flow waveforms and alters the configuration and velocity of flow throughout the arterial tree. Pulse patterns are distorted further by branching of the arterial tree, and by resistance to forward motion of flow (135). The result is that stiffness of the upstream arteries affects the downstream circulation through varying flow pattern, varying flow stress, and cellular responses and that changes in the distal resistance can influence proximal hydrodynamics through changes in operating pressure, smooth muscle cell (SMC)-mediated vessel stiffness, and over time, through changes in the passive material stiffness of the conduit vessels.

Mechanisms of Pulmonary Vascular Stiffening in Response to PH

Pulmonary vascular tissues have a complex, nonlinear, mechanical response, which relates tissue deformation to applied load. Changes in *in vivo* PVS are dependent on both the *in vivo* operating pressure as well as on changes in intrinsic artery material properties governed by the mechanics of structural proteins and the active contraction of SMCs and myofibroblasts. Passive mechanics of elastic arteries are typically characterized by a nonlinear force-stretch (F-λ) response which approximates a bilinear profile, Figure 5A. Here, force refers to the uniaxial load applied to a given tissue segment. In the case of artery inflation, this force is proportional to the hydrostatic pressure within the artery and is exerted as a tensile load applied in a direction tangent to the vessel circumference. Stretch (λ) refers to the normalized deformation of the tissue calculated as:

$$\lambda = \frac{L_{Deformed}}{L_{Gage}} \quad (7)$$

where $L_{Deformed}$ refers to the deformed length of the tissue and L_{Gage} refers to the gage length of the sample, which is typically equal to the configuration that the sample would assume under zero pressure load. In the case of a thin-walled tube of large diameter, an approximation which holds for the conduit arteries, the λ can most easily be thought of as the ratio of the artery circumference under a given pressure to the circumference of the artery at zero pressure.

The low-stretch region of the F-λ curve characterizes the mechanical properties of elastin, and is termed the elastin-dominant region (Fig. 5A). At some intermediate level of deformation, termed the transition stretch (λ_{Trans}), collagen begins to become engaged and able to carry part of the applied load. At stretches below λ_{Trans}, collagen, which is deposited in a coiled and wavy state in the unloaded configuration, is rotated and straightened in the direction of the applied load. Since the collagen is not yet aligned for stretch values below λ_{Trans}, it does not carry significant load within the elastin-dominant region. As the tissue is deformed to $\lambda > \lambda\lambda_{Trans}$, more of the load is carried by collagen, a material of high modulus which results in increased material stiffness within the transition region of the F-λ curve (130). Eventually, the majority of the collagen capable of carrying load in the direction of the applied deformation are oriented in a straightened and aligned configuration resulting in a second, roughly linear, F-λ region dominated by collagen mechanics (Fig. 5A).

PA stiffen in response to PH through at least three distinct mechanisms. The first stiffening mechanism is the change in intrinsic material properties of the arterial wall, Figure 5B. The second results from the extrinsic change in material stiffness due to the artery operating under conditions resulting in an elevated dilation, Figure 5C. And the third mechanism is that which is associated with the active contraction of arterial SMCs and/or myofibroblasts, Figure 5D.

Material property changes of the constituent structural proteins collagen and elastin (Fig. 5B) is the stiffening modality, which has received the most attention thus far. This is likely due to the fact that biological material characterization protocols are fairly well developed and lend themselves to quantitative experimental analysis as well as the fact that an understanding of passive mechanics is required before a thorough understanding of *in vivo* (i.e., dilation-induced) or SMC-mediated stiffening can be fully explored. During PH, both elastin and collagen are deposited within the extracellular matrix (ECM) of the large extrapulmonary arteries (67, 82, 134). The mechanical consequence of elastin and collagen deposition differ somewhat. An increase in elastin or a change in the cross-linking density of

the existing material will change the slope of the F-λ curve within the elastin dominant region (153, 154, 156). The linearity of the elastin F-λ curve will propagate this additional stiffness through the collagen dominant and transition regions as well, resulting in an constant increase in slope of the curve throughout its length (67, 160). Collagen-mediated mechanical changes impact the region of the F-λ curve at λ values greater than the transition stretch (λ_{Trans}). At λ values below λ_{Trans}, collagen is aligning/unfolding and is unable to carry significant loads within the elastin-dominant region (160). Collagen remodeling therefore affects the material stiffness of the transition and collagen-dominant regions, or may act to change the onset of collagen engagement by shifting the λ_{Trans}.

Total hydrodynamic capacitance of the pulmonary circulation is a function of both the extrapulmonary and elastic-intrapulmonary arteries. While significantly less progress has been made regarding PH-mediated histological and mechanical changes of the elastic-intrapulmonary arteries, evidence suggests that the physiological changes are similar between elastic intra and extrapulmonary arteries (53), however more research is needed to determine how PH vascular remodeling propagates through the more distal elastic arteries of the lung. The relative amounts of collagen and elastin deposited and concomitant changes in the PA F-λ curve differ somewhat between animal models. The hypoxic neonatal-calf model demonstrates a significant elastin-mediated PA stiffness elevation (67), the hypoxic adult mouse and rat stiffness elevation tends to be much more collagen-mediated (31, 64), the underlying reason for this difference is as of yet unknown. However, most PH animal models demonstrate a significant stiffness elevation within the conduit arteries responsible for hemodynamic capacitance.

Dilation-induced stiffening is an extrinsic stiffening modality which is dependent not on changes in tissue material properties but rather is a function of the operating condition of the pulmonary vascular system (Fig. 5C). Here, stiffening is the result of the tissue operating at elevated stretches, which moves the physiologic operating condition of the material from the low stiffness elastin-dominant region of the F-λ curve into the high-stiffness transition or collagen-dominant region. Typically this condition results from the system operating at the elevated pressures associated with hypertension, and can therefore be ameliorated by lowering the resistance of the pulmonary vascular bed.

PA material properties can be further changed through SMC activation, which results in elevated material stiffness throughout the elastin-dominant and transition regions of the F-λ curve (Fig. 5D). Measuring the effect of SMC activation on artery mechanics is complicated by the fact that in addition to changing vascular tone, active contraction alters the resting configuration of the tissue and is sensitive to environmental conditions, maximum and minimum stretch values, stretch rate and preconditioning. It is therefore somewhat more complicated to standardize testing protocols for measuring active PA tissue properties than for passive mechanics. This led to a significant difference in interpretation of the effect of arterial smooth muscle contraction on the elastic modulus of arterial tissues. Alexander (1, 41) found that elevated SMC activation resulted in decreased material modulus while Cox (25), Dobrin and Rovick (30), Barra et al. (5) found just the opposite. The reason for the disagreement is centered on the choice for the reference gage length used to calculate the material stretch. Stretch was defined in Eq. 7 as the ratio of the deformed length by the reference gage length of the unloaded sample. Therefore, changing the reference length between measurements will change the calculated λ of the sample for equally deformed lengths. Those who concluded that SMC activation resulted in decreased modulus used the low-pressure (i.e., 0–25 mmHg) artery circumference of each independent test as the reference gage length. Therefore, the active SMC F-λ referenced the low-pressure circumference of the actively contracting tissue as the gage length and the relaxed test referenced the relaxed initial configuration. In contrast, those who concluded that SMC

activation resulted in elevated modulus used a single reference gage length to calculate material stretch. The choice of the common reference gage length is somewhat arbitrary with Dobrin and Rovick choosing the circumference of the low-pressure actively contracting vessel while Cox and Barra chose to reference the passive low-pressure circumference as the gage length. Since the resting diameter of unloaded arteries is reduced by active SMC contraction, if the artery is deformed to the same dimensions the calculated stretch of the contracted tissue will be greater than that of the passive sample. However, if both tests reference a common gage length, then the calculated stretch will be equal. While both are accurate measures of material deformation, to compare the material properties of tissues at a given stretch, those tissues, which are to be compared, must reference the same gage length. Therefore, when discussing the effect that SMC activation has on the mechanics of arterial tissue it is more appropriate to discuss these changes in terms of the common reference gage length data, where SMC activation results in elevated stiffness across the elastin-dominant and transition regions of the F-λ curve. An intriguing additional possibility for how SMC contribute directly to vascular stiffening has been raised, intrinsic stiffening of the SMC themselves (118). This appears due to changes in the mechanical behavior of the actin cytoskeleton. This is interesting as increases in the stiffness of airway SMC have been related to the airflow abnormalities that characterize asthma (69).

While significant progress has been made in the understanding of how changes in elastin, collagen, and SMC tone affect the mechanics of PA in hypertensive subjects, disagreement remains with regard to the physiologic underpinnings and relative contribution of ECM components and SMC tone to artery mechanical properties. It is likely that much of this disagreement stems from comparisons made between results obtained from different animal models. Recent studies indicate that the cellular composition of the conduit arteries of the larger mammalian species (including cow, lamb, pig, and human) is more complex than that of the rodent species (132). These physiologic variations between the species naturally lead to differences in how the proximal arteries respond in hypertension. It is widely accepted that medial and adventitial thickening, associated with vascular remodeling, causes an increase in resistance due to the physical encroachment of the arterial lumen; however, recent studies indicate that the inhibition of Rho kinase, a small G-protein involved in SMC contraction, cell proliferation, and cytoskeletal rearrangement, nearly normalizes the hypertensive vascular resistance in both intact rats and perfused lungs for both acute and chronic administration of the inhibitor (57, 99, 133). This indicates that the hypertensive response of rodents is largely SMC based and that there is little significant inward remodeling of the arterial wall (34, 57, 99, 133). Calves respond differently and have been shown to demonstrate a loss of vasodilator response to acetylcholine, a potent neurotransmitter and vasodilator, within seven days of hypoxic exposure, indicating that vascular remodeling of calf arteries is more ECM dependent and that structural inward remodeling may occur on this model (32, 131, 133). In addition, the manner in which the large elastic PA of the calf and rat models respond to hypertension differs in the proliferation of SMCs and in the deposition of matrix proteins. It has been shown that the proximal PAs of larger mammalian species respond to hypertension through the activation of a distinct smooth-muscle-like cell subpopulation, which resides within the media (152). These smooth-muscle-like (or myofibroblast) cells may enable the large mammalian species to rapidly respond to hypertension by proliferating and secreting matrix proteins from these cells without first increasing the number of “synthetic” SMCs within the media, as seems necessary in the response of rodents to the disease (132).

A variety of other factors have also been implicated in vascular wall stiffening. Several genetic polymorphisms have been reported to influence PWV and thus aortic stiffening including those for the angiotensin I (AT1 receptor), fibrillin-1, metalloproteases, and endothelin (7, 66, 83, 84). In fact, aortic PWV and thus aortic stiffness appears to be a

heritable trait according to Framingham data (93). Age is also a significant determinant of stiffness and pulsatile hemodynamics. Stiffness, as noted, is related to the relative amounts of elastin and collagen in the vessel wall. It is now clear, at least in the systemic circulation, that collagen accumulates (relative to elastin) in the aorta with age and comorbidities, such as hypertension, diabetes, and cigarette use. It appears that long-term pulsatile stress leads to fragmentation of vascular elastin elements and accumulation of a collagen, with a loss of stretch and an increase in stiffness reflected by a steadily increasing systolic pressure (104). Previous work demonstrates that the same relationship may hold true for the pulmonary circulation (51). In addition, excessive accumulation of other proteins such as fibronectin, and desmin, also increase vascular stiffness (14). There also appears to be a relationship between sodium intake and vascular stiffness. There are instances in models of hypertension in which aortic stiffness results from increased salt intake independent of blood pressure changes (127). Diabetes also increases the aortic PWV, independent of other comorbidities or pathophysiologies. Whether this is true in the pulmonary circulation is unclear. Diabetes, however, has long been thought to be a model of accelerated aging and the accumulation of matrix materials, similar to that observed in aging in the vessel wall and their subsequent glycation has been speculated to be a principle mechanism of the effects of diabetes on aortic PWV (157).

Effects of Changes in Impedance on Ventricular Function

In order for the heart to supply blood flow to the vascular system, the heart must perform mechanical work on the blood. Mechanical work can be defined as the amount of energy transferred by a force, acting through a distance and power is defined as the rate at which work is done or energy is consumed. The energy transferred during a cardiac cycle of a pulsatile hemodynamic circuit comprises a pressure-dependent potential energy and a flow-dependent kinetic energy component. Further, the kinetic and potential energy can be further divided into a steady-flow and oscillatory component, and the total energy is simply the sum of these components. The energy thus imparted to the blood is primarily in the form of potential energy represented by the increase in fluid pressure, while a fraction is imparted as kinetic energy associated with the momentum of the ejected blood. In relation to the right ventricle, this mechanical work imparts the blood with enough total energy to complete one pass through the entire circuit of the pulmonary circulatory system terminating at the left atria. If the pressure (P) and flow (Q) are known over a given cardiac cycle, then the calculation of the stroke work is simply the integral of the pressure-volume product integrated over the time of one cardiac cycle:

$$W_{stroke} = \int_{t_0}^{T} PQdt \quad (8)$$

Where t_0 and T are the times corresponding to the beginning and end of one cardiac cycle. The work calculated using integration is of course not typically equal to the product of the mean values for pressure and flow averaged over the cardiac cycle ($\bar{P}$, $\bar{Q}$), respectively. The error associated with calculating the hydraulic work using the averaged values typically range from 10% to 30% less than the true value in the systemic circulation (86). However, this product of the mean pressure and flow is equal to the hydraulic power of a steady, nonpusatile, fluidic system operating at those mean conditions and is termed the steady flow power ($\dot{W}_S$).

$$\dot{W}_s = \bar{P} \cdot \bar{Q} \quad (9)$$

where $\dot{W}_S$ is a measure of steady-flow pressure-dependent potential energy of the pulmonary circulation. Since by definition $\dot{W}_S$ refers to steady-flow conditions this property

is largely determined by the vascular resistance and hence by the structure and activity of the microcirculation. If the input resistance is defined as

$$R_{in}=\frac{\bar{P}}{\bar{Q}} \quad (10)$$

then $\dot{W}_S$ can be rewritten in terms of pressure and resistance as

$$\dot{W}_S=\bar{Q}^2 R_{in}=\frac{\bar{P}^2}{R_{in}}. \quad (11)$$

Of course, the pulmonary circulation is not a steady flow system and therefore requires an additional parameter to account for the oscillatory power ($\dot{W}_O$) of the system. Given the periodic nature of pulmonary hemodynamics, $\dot{W}_O$ is best defined by the input impedance (Z_x) of the pulmonary circulation, a property, which was discussed in detail in the previous section on vascular impedance. For now, the input impedance can be thought of as the total resistance of an oscillatory system and is therefore analogous to R_{in} in a steady flow system. Z_x is a function of both the arterial compliance and the total downstream resistance of the pulmonary circulation. As discussed in the vascular impedance section, the pulsatile waveforms of arterial pressure and flow can be separated into their corresponding frequency components using Fourier analysis. These frequency components can then be used to calculate the oscillatory power using the equation

$$\dot{W}_O=\frac{1}{2}\sum_{n}^{N} Q_n^2 Z_n \cos\theta_n \quad (12)$$

where Q_n is the amplitude of the nth flow harmonic, Z_n and θ_n are the modulus and phase angle of the input impedance at the same harmonic frequency, respectively, and N is the total number of harmonics computed. The total pressure-dependent hydraulic power as pressure energy ($\dot{W}_T$) is the sum of the oscillatory and steady components

$$\dot{W}_T=\dot{W}_S=\dot{W}_O. \quad (13)$$

And the work associated with the pressure-dependent potential energy expended by the heart for each cardiac cycle ($W_{stroke,PE}$) can therefore be calculated using the equation

$$W_{stroke,\,PE}=\int_{t_0}^{T}\dot{W}_T(t)\,dt. \quad (14)$$

The kinetic energy associated with the cardiac cycle can be derived in similar fashion. Again, there is both a steady-flow and oscillatory component of the kinetic energy. Kinetic energy can be defined in the usual way as

$$K=\frac{1}{2}mv^2 \quad (15)$$

where m is the mass and v is the velocity of the fluid. In the above equation, it is assumed that the fluid velocity is uniform over the cross section of the flow stream (i.e., across the artery cross section). Therefore, the rate at which the kinetic energy of a fluid element ($d\dot{m}$) with a velocity (v) is transported through a differential area (dA) is:

$$K = \frac{1}{2} v^2 d\dot{m} \quad (16)$$

where $d\dot{m} = \rho v \cdot dA$. Taking the integral of K gives the total rate of transport of steady-flow kinetic energy through the cross section Awhich equals the steady flow kinetic power ($\dot{K}_S$)

$$\dot{K}_S = \int \frac{1}{2} v^2 dm = \frac{\rho}{2} \int v^3 dA. \quad (17)$$

If the fluid velocity is everywhere steady and uniform across the artery cross section, and is at a value equal to the average velocity, then the steady flow kinetic power simplifies to:

$$\dot{K}_S = \frac{\rho \bar{Q}^3}{2A^2} \quad (18)$$

where A is the cross-sectional area of the vessel lumen ($A = \pi R_i^2$).

The oscillatory part of the kinetic power can be calculated in a similar manner using a Fourier series representation of the flow, however, this approach results in fairly unwieldy equation of many terms. A simplified approach proposed by Milnor et al. was to calculate the total kinetic energy for a given pressure-flow pulse and then subtract the steady-flow component to find the oscillatory term (87). To accomplish this, the total kinetic power ($\dot{K}_T$) was calculated discretely using the equation where the flow

$$\dot{K}_T = \frac{\rho}{2A^2 J} \sum_{j=0}^{J} Q_j^3 \quad (19)$$

data was digitized with a time-interval Δt resulting in a total number of discrete observations J and a flow Q_j for each "j" observation. The oscillatory kinetic power is then equal to the difference between the steady-flow and total kinetic power:

$$\dot{K}_O = \dot{K}_T - \dot{K}_S. \quad (20)$$

In 1966 and 1969, Milnor et al. published data for the power requirements of the pulmonary circulation in dogs (87) and humans (88), respectively. The average power measurements presented in those publications are shown in Table 1.

The average power values tabulated in Table 1 represent the amount of work done on, or energy transferred to, the blood contained in the pulmonary circulation during one cardiac cycle. From Table 1, we find that the oscillatory component comprises approximately one-third of the total power requirement for the right ventricle to move blood through the pulmonary circulation while the steady flow component accounts for the remaining two-thirds of the total hydraulic power of healthy animals at rest. Other work has shown that in the systemic circulation the oscillatory component of hydrodynamic power accounts for only approximately 13% of the total hydraulic power requirement in healthy human subjects (102) and was reported to be less than 6% in the systemic circulation of healthy dogs (155).

The input hydraulic power is responsible for imparting enough energy to the blood volume contained within the pulmonary circulation to move forward a distance corresponding to the stroke volume of ejected blood. By the time the pressure-flow pulse has traveled the distance

from the main pulmonary artery (MPA) to the pulmonary vein, much of the energy contained within the initial pulse has been dissipated within the pulmonary bed. This power dissipation was measured by Milnor et al. in open-chest anesthetized dogs by recording both the input and output pulmonary hydraulic power and taking the difference between the two (87), the results of the tests are shown graphically in Figure 6. They found that nearly all of the oscillatory power and the majority of the steady-flow power were lost to resistive and reactive power dissipation within the pulmonary system.

The reactive power of the pulmonary circulatory system was measured in dogs to be approximately 10% of the total hydraulic input energy during systole (87). This reactive power, by definition, is the energy required to distend the conduit pulmonary artery walls. Since a portion of this energy will be returned to the system during diastole, the mean reactive power over the cardiac cycle is less than that measured during systole. In an ideal case, 100% of the reactive power would be returned during diastole. In reality, the phase relations of pressure and flow are interrupted by reflected waves, PWV, viscosity, and vascular structures resulting in less than ideal energy recovery. In any case, the total energy required to deform the arteries during systole is small and therefore may lead to the assumption that the effect of the reactive hydrodynamic power is negligible. However, any change in material properties of these capacitive arteries will change the overall hemodynamics and input impedance of the system and may significantly impact the total hydraulic power disproportionately to any associated change in the reactive energy required for direct vascular deformation.

As shown in Figure 6, the dissipation of hydraulic power throughout the pulmonary bed occurs within both the mean and oscillatory components of arterial blood flow. For a given mean blood flow, the mean hydraulic terms will, by definition, remain constant as will the mean power dissipation terms. However, the oscillatory terms of cardiac blood flow are functions of heart rate and, in turn, the oscillatory terms of hydraulic power dissipation are also heart rate dependent. Figure 7 details the change in power dissipation with respect to heart rate in anesthetized dogs where mean blood flow was held constant at 42.0 cm^3/s (87). In this figure, output power of the pulmonary circulation, measured at the pulmonary vein, is assumed to remain independent of heart rate; an assumption which is consistent with observations (87). The effect of this assumption is that any change in power dissipation is equal to a corresponding change in input power. Therefore, for a given mean flow the total input power is reduced by approximately one-half within the range of heart rate between 60 and 180 beats/min, and that at higher heart rates the overall input power remains relatively constant.

The coupled relationship between heart rate, stroke volume, mean blood flow, and hydraulic power of the pulmonary circulatory system appears to be in a balanced state in healthy dogs, and presumably in other healthy animals as well. This balance results in an ability to significantly increase the mean pulmonary blood flow with a very moderate increase in cardiac hydraulic power by elevating the heart rate and concurrently changing the pressure and flow waveforms to a more sinusoidal state. When mean blood flow is elevated through increased heart rate, the oscillatory component of arterial input power decreases but the steady component increases, resulting in a balance where total blood flow can be markedly elevated with very small changes in overall cardiac work requirements. This was tested in an experiment on open-chest dogs with surgically produced complete heart block and an artificial pacemaker to control heart rate. The results show that the increased heart rate and concomitant decrease in stroke volume acted to raise the pulmonary blood flow by 34% without any increase in input power (87). Of course in a traditional pipe-flow hydrodynamic system, the previous statement would be impossible; however, in the complex hydraulic system of the pulmonary circulation this result is empirically true as validated through

experimental results. Further, the above-mentioned study indicated that less input power was required to increase pulmonary blood flowthrough elevated heart rate than by an increase in stroke volume. This trend is more clearly evident in Figure 8, where the oscillatory component of hydraulic input power is plotted against the pulmonary blood flow for the three experimental conditions of increased heart rate at a constant stroke volume and three conditions of increased stroke volume at a constant heart rate. In the case where the heart rate remains constant and blood flow is increased by changing the stroke volume alone, the power will vary as the square of the mean flow (broken line). However, when the heart rate determines blood flow for a constant stroke volume the relationship between input power and flow is complicated by the fact that for any given flow rate the oscillatory component of input power decreases with increasing heart rate, as shown in Figure 7. The result is that pulmonary arterial blood flow can be more efficiently regulated through changes in heart rate than by equivalent changes in stroke volume for a substantial physiologic range of these values.

Of course, under ordinary conditions, neither heart rate nor stroke volume remains constant during changes in arterial blood flow. In the experiments with unanesthetized dogs performed by Milnor et al., they found that dogs at rest typically had a heart rate near 85 beats/min. Increased alertness was generally accompanied by an increase in heart rate to 100 to 120 beats/min and a corresponding increase in pulmonary blood flow of 20% to 35% with a slight decrease in stroke volume (87). In these experiments, the blood flow increased by nearly one-third, but there was little or no increase in total input power to the pulmonary circulation. However, while this energy saving mechanism operates efficiently under many physiological conditions, above a heart rate of approximately 160 further increases in blood flow no longer retain this heart rate-dependent efficiency. Further, it seems likely that this balance between heart rate, stroke volume, impedance, and input power could be easily upset by the changes in pulmonary circulatory hemodynamics and vascular mechanics associated with pulmonary vascular remodeling. While this subject has not yet been fully elucidated, further experiments have begun to shed light in how age-related changes in systemic vascular function impact cardiac mechanics during exercise.

In later experiments by Milnor et al., the effect of age and exercise on the ventricular-vascular coupling of systemic circulation were studied *in vivo* (155). They found that while at rest there were no differences in hemodynamic or derived aortic impedance parameters; however, even during mild exercise, there were profound differences in the hemodynamic response of the systemic vasculature and cardiac function. The results of these experiments are detailed in Figure 9. Figure 9A indicates that systolic volume increases with progressively strenuous exercise in young dogs. In senescent dogs, the stroke volume initially increased for mild exercise, however, there was not the same progressive elevation in this cardiac parameter with increased exercise as seen in the young animals. Figure 9B shows that while both young and old animals demonstrate similar levels of maximal reduction in vascular resistance in exercise, the old animals immediately react to mild exercise through a much larger decrease in vascular resistance compared to young dogs. Further, elevations in exercise levels do not result in a progressive decrease in vascular resistance in senescent animals, but do show that trend in young animals. Figure 9C shows a significant increase in characteristic impedance in the vessels of the old animals during mild exercise and a progressive elevation in impedance corresponding to increased exercise level. However, young animals show no significant elevation in characteristic impedance with exercise, a significantly different trend between the age groups. The increment in external power resulting from exercise is shown in Figure 9D. It is evident from these data that exercise results in increased hydraulic power exerted by the heart and that this increased power trends progressively upward with a corresponding elevation in exercise intensity.

However, it is also clear that aged dogs are less able to increase their total hydrodynamic power in response to exercise than are the young animals.

These results show that there is a profound difference in vascular response to exercise in the young and old animals studied. Further, while both groups show a similar magnitude in decreased vascular resistance, there are significant differences in both stroke volume and characteristic impedance changes between young and old animals in response to increased exercise levels. The result was that during severe exercise, the old dogs were only able to generate 65% of the cardiac output of young dogs. Stroke volume is decreased and/or ventricular afterload is increased when the vascular resistance or characteristic impedance are increased. In the case of exercise in senescent dogs, the resistance decreases while the characteristic impedance is increasing. Therefore the load components are altered in opposite directions and it is difficult to determine which component dominates the change in ventricular function. Studies, which use mechanical analogues of systemic vasculature, are in apparent disagreement with regard to the relative impact of resistance and capacitance changes to the resulting stroke volume. In two studies, it was shown that capacitance changes clearly dominated resistance in determining the changes in stroke volume (33, 58). However, other studies using a similar mechanical analogue showed exactly the opposite where resistance was shown to be the dominant factor (136, 137). Further, it appears that the specific isolated supported ventricle model itself, and imposed boundary conditions, may play a critical role in the measured relative contribution of resistive and capacitive changes on hydraulic function, and is an aspect, which will be considered in the following section.

Isolated supported ventricular models

Isolated supported ventricular models allow for the study of how changes in the variables which affect cardiac function, that is, heart rate, stroke volume, end diastolic and systolic volumes, distal resistance, and vascular compliance, affect the hemodynamics of the circulatory system. There are three isolated supported ventricular models used to investigate cardiac function *ex vivo*, which differ primarily in the inlet boundary condition supplying hydraulic fluid to the left ventricle. The first model uses a constant left-arterial-pressure inlet boundary condition and we will refer to this model as the pressure-controlled isolated supported ventricle (PCISV), Table 2. The second model uses an end-systolic/diastolic ventricular volume boundary condition and is referred to as the volume-controlled isolated supported ventricle (VCISV), Table 2. The third model is an adaptation of the VCISV in which a Windkessel model is used to impose a time-dependent ventricular flow based on a inlet pressure waveform, and is referred to as the Windkessel-controlled isolated supported ventricle (WCISV), Table 2. Of course, in these acronyms, controlled refers to the inlet boundary condition only and it is recognized that there are many other input variables used to control and study these systems.

Supported ventricular systems consist of an *ex vivo* heart supported by a secondary living animal, which supplies blood to the coronary artery of the isolated heart being tested. This removes any dependence of coronary artery perfusion on isolated ventricular blood flow, an effect, which would likely otherwise affect cardiac contractility. The isolated heart, thus supplied with a constant supply of coronary blood, was also connected to an artificial pacemaker so that the heart rate could be controlled.

VCISV and PCISV systems differ significantly in both their mechanical analog to distal vascular resistance and compliance as well as a difference in inlet boundary conditions (Figures 10 and 11). The PCISV uses a constant left atrial filling pressure supplied by a pressurized hydraulic reservoir. The inlet boundary condition of the VCISV is the end-systolic and/or end diastolic ventricular volume imposed by a piston pump through a balloon inserted into the left ventricle (137). Several differences exist between the mechanical

analogs of distal resistance and arterial compliance represented by the two isolated supported ventricle models. First, the VCISV does not circulate fluid but rather moves the same fluid volume between the ventricle and the piston pump whereas the PCISV does move fluid through a mechanical analog of vascular circulation. Second, the VCISV does not have any ventricular valves nor any functional atria, allowing for control of the onset of ejection timing with respect to the initiation of systole at the expense of the *in vivo* hydrodynamics of the aortic valve, which are retained in the PCISV model. In the VCISV model, end systolic and end diastolic volumes could be set and fixed at given values. Further, the pressure against which the ventricle was ejecting blood was controlled by a preprogrammed command signal of volume as a function of time. In the case of the PCISV, the end systolic and end diastolic volumes could not be directly controlled and were therefore dependent on the inlet pressure and imposed afterload of the mechanical analog representing the distal resistance and arterial compliance of the systemic circulation.

The experiments performed by Suga et al. in their comprehensive study of the VCISV model, indicate that the endsystolic volume is a very strong function of end-systolic pressure, end-diastolic volume, and contractile state but is not a strong function of the particular pressure/volume course taken between end-diastolic and end-systolic conditions (136). Several limitations exist for the VCISV model with regard to its accurate representation of *in situ* ventricular-vascular coupling and cardiac hydrodynamics. Most importantly is the fact that *in vivo* end-systolic pressure is not fixed and is variable with changes in end-diastolic state and arterial impedance. To address this limitation within the framework of the isolated supported ventricle model, the VCISV was adapted to utilize a feedback control system, based on a Windkessel electrical analogue, to model ventricular-vascular coupling and overall systemic hemodynamics. A diagram of this WCISV model system is shown in Figure 12. In the WCISV, an electrical analog of a three-element Windkessel arterial model was used to generate the time-dependent ventricular flow(i.e., flow waveform) from an input time-dependent ventricular pressure (i.e., pressure waveform). Therefore, by using the Windkessel model, the WCISV system can impose an instantaneous flow based on characteristic impedance, arterial compliance, and distal resistance and an input pressure wave.

The results of the WCISV model used by Sunagawa et al., are shown in Figure 13, where the values for the distal resistance and/or arterial compliance were changed from 50% to 200% of control conditions and *P-V* loops were acquired at four different end-diastolic volumes for each of the nine experimental resistance/compliance permutations. Within the tested range, the resistance of the system was significantly more important than the arterial compliance in determining the change in stroke volume, Figure 13 (148). Further, the ratio of end-systolic pressure to stroke volume was highly dependent on resistance changes while being relatively independent of any change in compliance, Figure 13, panels B and C. Upon inspection of panel A in Figure 13, it is clear that the *P-V* loops changed shape only to a modest degree under the experiments where the compliance was varied, typically only demonstrating a flattening of the systolic pressure curve. However, changes in distal resistance resulted in much more dramatic changes in overall *P-V* loop shape at the given end-diastolic conditions. The obvious conclusion of this result would be to assume that changes in compliance have very little effect on the cardiac hemodynamics directly related to the work that the heart must perform on the blood to move it through the circulation. It should be noted that this conclusion was not stated in Sunagawa et al., but it is easily the conclusion one could draw from the given information. However, this conclusion is in stark contrast to the one indicated by the relationship between age and disease mentioned previously (155) and is in direct contradiction to the results of the experiments using the PCISV models discussed below.

The PCISV model, shown in Figure 10 uses a constant left-arterial-pressure inlet boundary condition instead of the prescribed stroke volumes used in the VCISV and WCISV models. The PCISV model differs from the volume-controlled models in two other significant ways. First, the pumping fluid enters the ventricle through the left atria instead of through the reversal of flow at the mitral outlet used in the volume-controlled models. Second, unlike the WCISV model, which used a Windkessel model to generate a cardiac blood flow profile, which was imposed on the ventricle through the piston pump, the PCISV uses physical compliance and resistance chambers to impose different afterload conditions upon the left ventricle directly. When the afterload variables of distal resistance and vascular compliance were varied in the PCISV model the resulting left ventricular pressure (LVP), aortic flow, and aortic pressures were quite different than those resulting from the WCISV model under similar interrogation of afterload-dependent variables.

Using a PCISV model of a cat left ventricle, Elzinga and Westerhof measured changes in hemodynamic and cardiac parameters resulting from changes in the afterload-dependent variables of distal resistance and aortic compliance (33). Typical results for LVP, aortic pressure, and aortic flow measured for the nine experimental conditions are shown in Figure 14 where situation 1 is the control condition. A decrease in compliance (situations 1, 4, and 7) and an increase in resistance (situations 1, 2, and 3) both resulted in increased systolic LVP, Figure 14. Comparison between situations 4 and 7 indicates that a stiffer system results in a more triangular LVP waveform and that increasing resistance did not change the typical square-wave nature of the LVP signal. The results for the aortic pressure show a strong relationship with loading conditions. Increased resistance resulted in an elevation of the mean aortic pressure but only a small change in pulse pressure. Decreased compliance, however, resulted in a decrease in the mean aortic pressure with a significant increase in pulse pressure. Aortic flow was also significantly influenced by afterload conditions. Peak systolic flow and stroke volume both decreased with either rising distal resistance or decreased aortic compliance, however these effects were more pronounced with changes in stiffness.

Results for aggregated data from six feline PCISV hearts exposed to a 208% increase in resistance and a 21% decrease in compliance are given in Table 3. Similar results were obtained for changes in the resistance and compliance parameters of PCISV hearts from dogs (58). The PCISV model results indicate a significant relationship between aortic compliance and systemic circulatory hemodynamics. In particular, this model indicates that for even relatively small changes in compliance (21%, Table 3) the effect on relevant hemodynamic parameters such as pulse pressure and stroke volume are equivalent to the changes in those variables associated with much larger increase in distal resistance (208%, Table 3). Further, the changes in the pressure and flow waveforms resulting from decreased arterial compliance can be quite dramatic, Figure 14.

All of the results presented thus far for isolated supported ventricles specifically model the systemic circulation only. The oscillatory power component of the pulmonary circulation is approximately 30% to 40% of the total power. In the systemic circulation the oscillatory power component is only approximately 5–15% of the total power. Therefore, it stands to reason that the impact of decreased arterial compliance may even be more important in determining the circulatory hemodynamics of the pulmonary circulation than the systemic circulation. As mentioned previously, there are numerous coupled system parameters upon which circulatory hemodynamics and cardiac function are dependent. The VCISV and WCISV systems assume constant contractility (i.e., constant end-systolic pressure—volume relationship) and impose an end-diastolic and end-systolic pressure or volume boundary condition, which is not necessarily representative of the response of the in-situ system to equivalent changes in resistance or compliance. As such, these models do a good job of

investigating the impact of end-systolic and end-diastolic volumes on the hemodynamic and cardiac functions of the systemic circulation, but does not capture the relationship between compliance or resistance on the resultant *in situ* stroke volume of the system. The PCISV model allows for the system to operate in a more native manner by allowing the stroke volume to change in response to a change in afterload conditions. This allows for the model to better capture the *in situ* response of the circulatory system at the expense of direct control of the stroke volume. Therefore, the PCISV is likely to produce results that more closely match the *in situ* response of the system to changes in arterial compliance and distal resistance. While further study is clearly warranted to define the response of the pulmonary circulation to changes in afterload, it seems likely that changes in characteristic impedance have a significant impact on stroke volume and cardiac function of the pulmonary circulation.

Effects of Proximal Arterial Stiffening on the Distal Pulmonary Circulation

Besides being a conduit between heart and arterioles, the large elastic arteries act as a dashpot, transforming pulsatile flow at the large elastic arteries into near steady flow through the more distal vasculature. Normally, these tasks are so efficiently performed that the mean pressure in the ascending aorta is only 1 to 2 mmHg greater than in a peripheral blood vessel such as the radial artery (110, 111). Mean pressure is thus maintained throughout the whole arterial tree while pulsatility around the mean in the large elastic arteries is minimized. Recent careful measurements by Christensen and Mulvany suggest that pulse pressure is transmitted much deeper into the microcirculation than was previously believed, especially in vasodilated beds (24). The same was found in the pulmonary circulation (46). Proximal stiffening could significantly increase the transmission of high-energy pulse waves into the microcirculation of the lung. However, there has been a distinct lack of study evaluating the possibility that proximal pulmonary arterial wall stiffening, which causes increases in pulse pressure and PWV, contributes to the pathologic abnormalities in the distal PA that characterize chronic PH. This is curious given the fact that interest in the role that aortic stiffening plays in the pathogenesis of cardiovascular disease has increased dramatically, in large part because of studies that have used either pulse pressure or PWV as a measure of stiffness. Numerous studies performed over the past decade have shown that higher pulse pressure is associated with moderate but significant increases in the risk for major cardiovascular disease events, such as myocardial infarction, heart failure, arrhythmia, and stroke (16, 37, 93). In addition, there is now good evidence that excessive pressure pulsatility is associated with and probably causes microvascular damage and dysfunction, which helps to explain the associations between aortic stiffness, increased pulse pressure, and a number of conditions thought to involve microvascular insult such as chronic kidney disease, cognitive impairment and Alzheimer disease, macular disease of the eye, and white matter lesions of the brain (63, 68, 89, 90, 125). The organs most affected by arterial stiffening and thus changes in pulse pressure and PWV, are high-flow, low-impedance organs, like the brain and kidneys. In these organs, pressure pulsatility penetrates further into the microcirculation thereby exposing small arteries and capillaries to damaging levels of pressure pulsatility. The relationship of arterial stiffness to abnormalities in kidney function is well studied and has recently been reviewed by Safar et al. (125). It has been consistently demonstrated that high pulse pressure is associated with reduced kidney function as assessed by glomerular filtration rate and is associated with accelerated decline in kidney function over time. Aortic stiffening has also been associated with albuminuria, a marker of microvascular kidney damage.

In the brain, another high-flow low-impedance organ, cerebral microbleeds, characterized by localized hemosiderin deposits, are increased in proportion to pulse pressure (147). Silent cortical and subcortical infarcts have also been related to pulse pressure (146). A

relationship between pulse pressure and cognitive impairment has also been established. For instance, white matter lesions in the brain as assessed by time-weighted MRI scans, are increasingly prevalent with age and are associated with impaired cognitive function (43). White matter lesions are thought to reflect cumulative adverse effects of microvascular dysfunction, impaired autoregulation and intermittent relative ischemia. Indeed, pathologic studies reveal arteriosclerotic changes in small vessels in regions with white matter lesions, with deposition of hyaline material in a thickened media, reduced internal diameter and markedly increased media to lumen ratio (109). It is also important to note that chronic kidney disease, microvascular brain pathology, and cognitive impairment cocluster suggesting shared mechanisms in pathogenesis. The common association with pulse pressure suggests a relationship or causal role for aortic stiffness. Recent studies have begun to explore more specifically this relationship (149).

Mechanistic insight into these important clinical findings relating proximal (aortic) stiffness to microvascular dysfunction, have been increasingly evaluated in both humans and animal models. Several studies demonstrate that microvascular endothelial function, vascular remodeling, and myogenic tone may be more sensitive to alterations in pulse pressure than mean arterial pressure (MAP) (15, 23). These studies and others have led to the speculation that hypertrophic remodeling and increased tone in the microcirculation, in response to excessive pressure pulsatility, may represent a mechanism whereby a primary abnormality in aortic stiffness and pressure could promote secondary elevation of MAP cumulating in a feedback system, which results in systolic hypertension. Mitchell et al. tested this hypothesis, that large artery stiffness has a direct effect on microvascular structure and function, by testing the relation between aortic stiffness and forearm microvascular function as reported in the Framingham Offspring Cohort (94). They found that vascular resistance measured in the forearm was increased moderately at rest and markedly during hyperemia in proportion to the stiffness of the aorta (measured in terms of both PWV and pulse wave amplitude). In support of these findings are additional population based studies showing that the diameter of retinal arterioles was reduced in individuals with a stiff aorta or carotid artery (20).

These recent studies have gradually brought to light some basic knowledge of the concepts as to how the pulsatility modulation function of elastic arteries is disordered in hypertension. One emerging concept is that wave propagation in the arterial system indicates strong interactions between large arteries (macrocirculation) and the microvascular network (microcirculation). Along the arterial tree of the systemic circulation, elastic arteries buffer the flow wave pulsations, muscular arteries actively alter wave propagation velocity and arterioles serve as major wave reflection sites (122). Each of these alterations (or their combination) enables a crosstalk between the proximal and distal compartments of the arterial tree (75, 80, 101, 123). Optimal arterial function requires appropriately distensible proximal arteries, appropriately timed wave reflections, and an appropriate heart rate and ejection duration (122). The pulmonary circulation, however, is characterized with little wave reflection, because of its low resistance and high compliance (50, 98). Therefore, the impact of the compliance of proximal arteries and the rate and ejection duration of the right ventricle on the actions of pulmonary muscular arteries and arterioles are likely more important. PH, as well as normal aging, leads to increases in proximal stiffness and in PWV and pulsatility in the pulmonary circulation. Forward wave amplitude serves as an indicator of the potential energy of the waveform, which can be transmitted to the distal circulation. PWV represents a marker of waveform momentum or kinetic energy. Elevation of either component can enhance transmission of pulsatile energy into the microcirculation, leading to activation of mechanosensitive genes, increased oxidative stress, and altered structure and function. While *in vivo* studies have been central to establishing physiologic and pathophysiologic roles of perfusion pulsatility, they could not delineate the relative

importance of the different mechanical forces (i.e., shear vs. stretch) and could not address the importance of the relative balance of these forces. The relative balance is important because vascular diseases such as hypertension can significantly influence different mechanical forces imposed on the vascular cells with what appears to be the same pulse pressure (122).

Arterial flow is pulsatile, exposing the vessel wall to phasic nonreversing changes in wall shear stress in combination with compressive pressure and tensile stress due to distension. Each form of mechanical force is known to be a potent stimulus for endothelial regulation of smooth muscle tone, cellular growth and apoptosis, monocyte adhesion, and other factors. The majority of studies establishing the key mechanotransduction signaling mechanisms underlying the effects of shear stress or stretch have imposed steady stimulations focusing on elaborating the magnitude in mean values. Some have studied oscillatory/reversing changes in shear stress. Few have imposed pulsatile nonreversing changes in shear stress, and even fewer have combined all stimuli as occurs *in vivo*. Kass et al. have pioneered the research of imposing all stimuli exhibited in the physiologically relevant pulse waveform on endothelial cells to study the cytoprotective effects of flow (71, 113). In elastic arteries, different forces more synergistically regulate vascular cell function; in stiffer or distal arteries, tensile stress is diminished because of reduced wall motion, and higher pulsatile shear stress together with pressure is imposed on the endothelium. The endothelium, uniquely situated at the interface between the blood and the vessel wall, is effectively a complex biological mechanotransducer that senses flow shear forces, converts these physical stimuli to biochemical signals, regulates vessel tone and alters vascular remodeling. The mechanotransduction mechanisms have been reviewed by Davies, Chien, and others (21, 22, 26–28, 42). These in-depth reviews have provided evidence of the ability of endothelial cells not only to sense shear stress, but also to discriminate among distinct types of flow patterns. They have also shown that hemodynamic stresses in the vascular system are under strict regulation and that a narrow homeostatic range of stresses exists where even a small perturbation of mechanical homeostasis may lead to activation of adverse signaling events in the endothelium, which ultimately result in abnormal vascular remodeling (21, 62).

To more quantitatively describe the pulsatility of arterial flow, pulsatility was recently quantified by using energy-equivalent pressure (EEP) and surplus hemodynamic energy (SHE), the critical contributor to hemodynamic energy besides mean pressure values in the studies related to assisted ventricle devices (60, 141, 144). These metrics calculated from hemodynamic waveform measurements have been shown to provide a more physiologically relevant measure of pulsatility than the commonly reported pulse pressure. The flow waveforms can be converted from time to frequency domain by using Fourier analysis algorithms. The EEP formula is defined as the ratio of the area beneath the hemodynamic power curve ($\int f p dt$) to the area beneath the pump flow curve ($\int f dt$) during each pulse cycle or, alternatively, the hemodynamic energy per unit volume of fluid pumped. It was calculated as follows: $EEP = (\int f p dt)/(\int f dt)$, where f is the pump flow rate (in liters per minute), p is the arterial pressure (in millimeters of mercury), and dt indicates that the integration is performed over time (t). The units for the EEP are millimeters of mercury, and as such, it is possible to compare the EEP with the MAP. The SHE value is calculated by multiplying the difference between the EEP and MAP values by the conversion factor 1332 as follows: $\mathrm{SHE(ergs/cm^3)} = 1332\ [((\int f p dt)/(\int f dt)) - \mathrm{MAP}]$. This represents the extra energy required for generation of pulse flow in terms of energy (not pressure) units and is thus a physiologically relevant measure of pulsatility because the generation of pulse flow in the body is dependent on an energy gradient rather than a pressure gradient.

To explore the possibility that the pulsatility modulation function of stiffened pulmonary large arteries is impaired and may lead to adverse remodeling of pulmonary

microvasculature due to greater energy dissipation across the distal “resistance” vessels (Fig. 15), our group developed a modified flow system that could be utilized to generated pulse waves of varying magnitude and investigated the effect of flow pulsatility on the pulmonary microvascular endothelium (73). EEP and SHE were calculated to determine the appropriate pulsatility imposed in the system and quantitative analysis of flow waveforms were used to connect the flow settings in vitro with hydrodynamic measurements *in vivo* (Fig. 16). It was shown that high pulsatility flow had significantly different effects than steady flow on a wide variety of inflammatory markers in endothelial cells. High pulsatility flow was shown to activate proinflammatory genes including ICAM, E-selectin, and MCP-1 in pulmonary microvascular endothelial cells. Genes related to endothelial proliferation, VEGF, and Flt- 1, were also upregulated. Importantly, these mRNA changes were accompanied by increases in monocyte adhesion to endothelial cells that had been exposed to high pulsatility flow (73).

Collectively, studies in the pulmonary circulation suggest a distinct separation of the effects of flow pulsatility from the effects of flow magnitude or flow turbulence. They support the concept that changes in the large vessel stiffness leads to changes in the propagation of high-energy pulsatile waves which are transmitted to the microcirculation, this could perpetuate or potentially even cause the microcirculatory changes so frequently observed in PH. The idea that large vessel stiffening may be important in the early stages of PH has recently been raised by studies showing that changes in indices of proximal vascular stiffening, as detected by the use of MRI scans, can be observed in patients with exercise and these increases in pulsatility are noted prior to any increases in resting mean pulmonary arterial pressures (128). Future work should be directed at evaluating the effects of high-energy pulsatile flow, as generated by stiff proximal PA, in the development and/or perpetuation of the structural remodeling and functional abnormalities that characterize PH.

References

1. Alexander RS. The influence of constrictor drugs on the distensibility of the splanchnic venous system, analyzed on the basis of an aortic model. Circ Res. 1954; 2:140–147. [PubMed: 13141377]
2. Avolio AP, Chen SG, Wang RP, Zhang CL, Li MF, O’Rourke MF. Effects of aging on changing arterial compliance and left ventricular load in a northern Chinese urban community. Circulation. 1983; 68:50–58. [PubMed: 6851054]
3. Badesch DB, Champion HC, Sanchez MA, Hoeper MM, Loyd JE, Manes A, McGoon M, Naeije R, Olschewski H, Oudiz RJ, Torbicki A. Diagnosis and assessment of pulmonary arterial hypertension. J Am Coll Cardiol. 2009; 54:S55–S66. [PubMed: 19555859]
4. Balzer DT, Kort HW, Day RW, Corneli HM, Kovalchin JP, Cannon BC, Kaine SF, Ivy DD, Webber SA, Rothman A, Ross RD, Aggarwal S, Takahashi M, Waldman JD. Inhaled nitric oxide as a preoperative test (INOP test I): The INOP Test Study Group. Circulation. 2002; 106:I76–I81. [PubMed: 12354713]
5. Barra JG, Armentano RL, Levenson J, Fischer EI, Pichel RH, Simon A. Assessment of smooth muscle contribution to descending thoracic aortic elastic mechanics in conscious dogs. Circ Res. 1993; 73:1040–1050. [PubMed: 8222076]
6. Barst RJ, McGoon M, Torbicki A, Sitbon O, Krowka MJ, Olschewski H, Gaine S. Diagnosis and differential assessment of pulmonary arterial hypertension. J Am Coll Cardiol. 2004; 43:40S–47S. [PubMed: 15194177]
7. Benetos A, Gautier S, Ricard S, Topouchian J, Asmar R, Poirier O, Larosa E, Guize L, Safar M, Soubrier F, Cambien F. Influence of angiotensin-converting enzyme and angiotensin II type 1 receptor gene polymorphisms on aortic stiffness in normotensive and hypertensive patients. Circulation. 1996; 94:698–703. [PubMed: 8772690]
8. Levy BI. Artery changes with aging: Degeneration or adaption? Dial Cardio Med. 2001; 6:104–111. 117.

9. Blacher J, Asmar R, Djane S, London GM, Safar ME. Aortic pulse wave velocity as a marker of cardiovascular risk in hypertensive patients. Hypertension. 1999; 33:1111–1117. [PubMed: 10334796]
10. Borlaug BA, Kass DA. Invasive hemodynamic assessment in heart failure. Heart Fail Clin. 2009; 5:217–228. [PubMed: 19249690]
11. Bradlow WM, Gatehouse PD, Hughes RL, O'Brien AB, Gibbs JS, Firmin DN, Mohiaddin RH. Assessing normal pulse wave velocity in the proximal pulmonary arteries using transit time: A feasibility, repeatability, and observer reproducibility study by cardiovascular magnetic resonance. J Magn Reson Imaging. 2007; 25:974–981. [PubMed: 17457797]
12. Budhiraja R, Tuder RM, Hassoun PM. Endothelial dysfunction in pulmonary hypertension. Circulation. 2004; 109:159–165. [PubMed: 14734504]
13. Castelain V, Herve P, Lecarpentier Y, Duroux P, Simonneau G, Chemla D. Pulmonary artery pulse pressure and wave reflection in chronic pulmonary thromboembolism and primary pulmonary hypertension. J Am Coll Cardiol. 2001; 37:1085–1092. [PubMed: 11263613]
14. Cattan V, Kakou A, Louis H, Lacolley P. Pathophysiology, genetic, and therapy of arterial stiffness. Biomed Mater Eng. 2006; 16:S155–S161. [PubMed: 16823107]
15. Ceravolo R, Maio R, Pujia A, Sciacqua A, Ventura G, Costa MC, Sesti G, Perticone F. Pulse pressure and endothelial dysfunction in never-treated hypertensive patients. J Am Coll Cardiol. 2003; 41:1753–1758. [PubMed: 12767660]
16. Chae CU, Pfeffer MA, Glynn RJ, Mitchell GF, Taylor JO, Hennekens CH. Increased pulse pressure and risk of heart failure in the elderly. JAMA. 1999; 281:634–639. [PubMed: 10029125]
17. Champion HC, Michelakis ED, Hassoun PM. Comprehensive invasive and noninvasive approach to the right ventricle-pulmonary circulation unit: State of the art and clinical and research implications. Circulation. 2009; 120:992–1007. [PubMed: 19752350]
18. Chemla D, Castelain V, Herve P, Lecarpentier Y, Brimioulle S. Haemo-dynamic evaluation of pulmonary hypertension. Eur Respir J. 2002; 20:1314–1331. [PubMed: 12449189]
19. Chesler NC, Roldan A, Vanderpool RR, Naeije R. How to measure pulmonary vascular and right ventricular function. Conf Proc IEEE Eng Med Biol Soc. 2009; 2009:177–180. [PubMed: 19964469]
20. Cheung N, Sharrett AR, Klein R, Criqui MH, Islam FM, Macura KJ, Cotch MF, Klein BE, Wong TY. Aortic distensibility and retinal arteriolar narrowing: The multi-ethnic study of atherosclerosis. Hypertension. 2007; 50:617–622. [PubMed: 17698721]
21. Chien S. Mechanotransduction and endothelial cell homeostasis: The wisdom of the cell. Am J Physiol Heart Circ Physiol. 2007; 292:H1209–H1224. [PubMed: 17098825]
22. Chien S. Effects of disturbed flow on endothelial cells. Ann Biomed Eng. 2008; 36:554–562. [PubMed: 18172767]
23. Christensen KL. Reducing pulse pressure in hypertension may normalize small artery structure. Hypertension. 1991; 18:722–727. [PubMed: 1835958]
24. Christensen KL, Mulvany MJ. Location of resistance arteries. J Vasc Res. 2001; 38:1–12. [PubMed: 11173989]
25. Cox RH. Mechanics of canine iliac artery smooth muscle in vitro. Am J Physiol. 1976; 230:462–470. [PubMed: 1259026]
26. Davies PF. Endothelial transcriptome profiles in vivo in complex arterial flow fields. Ann Biomed Eng. 2008; 36:563–570. [PubMed: 17978875]
27. Davies PF. Hemodynamic shear stress and the endothelium in cardiovascular pathophysiology. Nat Clin Pract Cardiovasc Med. 2009; 6:16–26. [PubMed: 19029993]
28. Davies PF, Spaan JA, Krams R. Shear stress biology of the endothelium. Ann Biomed Eng. 2005; 33:1714–1718. [PubMed: 16389518]
29. DeLoach SS, Townsend RR. Vascular stiffness: Its measurement and significance for epidemiologic and outcome studies. Clin J Am Soc Nephrol. 2008; 3:184–192. [PubMed: 18178784]
30. Dobrin PB, Rovick AA. Influence of vascular smooth muscle on contractile mechanics and elasticity of arteries. Am J Physiol. 1969; 217:1644–1651. [PubMed: 5353039]

31. Drexler ES, Quinn TP, Slifka AJ, McCowan CN, Bischoff JE, Wright JE, Ivy DD, Shandas R. Comparison of mechanical behavior among the extrapulmonary arteries from rats. J Biomech. 2007; 40:812–819. [PubMed: 16682044]
32. Durmowicz AG, Orton EC, Stenmark KR. Progressive loss of vasodilator responsive component of pulmonary hypertension in neonatal calves exposed to 4,570 m. Am J Physiol. 1993; 265:H2175–H2183. [PubMed: 8285257]
33. Elzinga G, Westerhof N. Pressure and flow generated by the left ventricle against different impedances. Circ Res. 1973; 32:178–186. [PubMed: 4685962]
34. Fagan KA, Oka M, Bauer NR, Gebb SA, Ivy DD, Morris KG, McMurtry IF. Attenuation of acute hypoxic pulmonary vasoconstriction and hypoxic pulmonary hypertension in mice by inhibition of Rho-kinase. Am J Physiol Lung Cell Mol Physiol. 2004; 287:L656–L664. [PubMed: 14977625]
35. Feihl F, Liaudet L, Waeber B. The macrocirculation and microcirculation of hypertension. Curr Hypertens Rep. 2009; 11:182–189. [PubMed: 19442327]
36. Finkelstein SM, Collins VR, Cohn JN. Arterial vascular compliance response to vasodilators by Fourier and pulse contour analysis. Hypertension. 1988; 12:380–387. [PubMed: 3169948]
37. Franklin SS, Khan SA, Wong ND, Larson MG, Levy D. Is pulse pressure useful in predicting risk for coronary heart Disease? The Framingham heart study. Circulation. 1999; 100:354–360. [PubMed: 10421594]
38. Galie N, Manes A, Negro L, Palazzini M, Bacchi-Reggiani ML, Branzi A. A meta-analysis of randomized controlled trials in pulmonary arterial hypertension. Eur Heart J. 2009; 30:394–403. [PubMed: 19155250]
39. Galie N, Simonneau G, Barst RJ, Badesch D, Rubin L. Clinical worsening in trials of pulmonary arterial hypertension: Results and implications. Curr Opin Pulm Med. 2010; 16(Suppl 1):S11–S19. [PubMed: 20375660]
40. Gan CT, Lankhaar JW, Westerhof N, Marcus JT, Becker A, Twisk JW, Boonstra A, Postmus PE, Vonk-Noordegraaf A. Noninvasively assessed pulmonary artery stiffness predicts mortality in pulmonary arterial hypertension. Chest. 2007; 132:1906–1912. [PubMed: 17989161]
41. Gao F, Liao D, Drewes AM, Gregersen H. Modelling the elastin, collagen and smooth muscle contribution to the duodenal mechanical behavior in patients with systemic sclerosis. Neurogastroenterol Motil. 2009; 21:914–e968. [PubMed: 19413680]
42. Garcia-Cardena G, Comander J, Anderson KR, Blackman BR, Gimbrone MA Jr. Biomechanical activation of vascular endothelium as a determinant of its functional phenotype. Proc Natl Acad Sci U S A. 2001; 98:4478–4485. [PubMed: 11296290]
43. Garde E, Mortensen EL, Krabbe K, Rostrup E, Larsson HB. Relation between age-related decline in intelligence and cerebral white-matter hyperintensities in healthy octogenarians: A longitudinal study. Lancet. 2000; 356:628–634. [PubMed: 10968435]
44. Gow, B. Circulatory correlates: Vascular impedance, resistance, and capacity. Comprehensive Physiology. John Wiley & Sons, Inc.; 1980. p. 353-408.
45. Guerin AP, Blacher J, Pannier B, Marchais SJ, Safar ME, London GM. Impact of aortic stiffness attenuation on survival of patients in end-stage renal failure. Circulation. 2001; 103:987–992. [PubMed: 11181474]
46. Guntheroth WG, Gould R, Butler J, Kinnen E. Pulsatile flow in pulmonary artery, capillary, and vein in the dog. Cardiovasc Res. 1974; 8:330–337. [PubMed: 4278240]
47. Guyton, AC. Medical Physiology. Schmitt, W., editor. Philadelphia: Saunders; 2000.
48. Hall, J.; Schmidt, G.; Wood, L.; Taylor, C. Principles of Critical Care. Hall, JB.; Schmidt, GA.; Wood, LDH., editors. New York: McGraw-Hill; 2005.
49. Haneda T, Nakajima T, Shirato K, Onodera S, Takishima T. Effects of oxygen breathing on pulmonary vascular input impedance in patients with pulmonary hypertension. Chest. 1983; 83:520–527. [PubMed: 6825485]
50. Hardziyenka M, Reesink HJ, Bouma BJ, de Bruin-Bon HA, Campian ME, Tanck MW, van den Brink RB, Kloek JJ, Tan HL, Bresser P. A novel echocardiographic predictor of in-hospital mortality and midterm haemodynamic improvement after pulmonary endarterectomy for chronic thrombo-embolic pulmonary hypertension. Eur Heart J. 2007; 28:842–849. [PubMed: 17341501]

51. Harris P, Heath D, Apostolopoulos A. Extensibility of the human pulmonary trunk. Br Heart J. 1965; 27:651–659. [PubMed: 5829747]
52. Howell, W. Textbook of Physiology Excitable Cells and Neurophysiology. 21st ed. Patton, Harry D.; Fuchs, Albert F.; Hille, Bertil; Scher, Allen M.; Steiner, Robert, editors. Philadelphia: W.B. Saunders; 1989.
53. Huang PJ, Chien KL, Chen MF, Lai LP, Chiang FT. Efficacy and safety of imidapril in patients with essential hypertension: A double-blind comparison with captopril. Cardiology. 2001; 95:146–150. [PubMed: 11474160]
54. Huez S, Brimioulle S, Naeije R, Vachiery JL. Feasibility of routine pulmonary arterial impedance measurements in pulmonary hypertension. Chest. 2004; 125:2121–2128. [PubMed: 15189931]
55. Hughes, JMB.; Morrell, NW. Pulmonary Circulation: From Basic Mechanisms to Clinical Practice. Anderson, Robert H., editor. London: Imperial College Press; 2001.
56. Hunter KS, Lee PF, Lanning CJ, Ivy DD, Kirby KS, Claussen LR, Chan KC, Shandas R. Pulmonary vascular input impedance is a combined measure of pulmonary vascular resistance and stiffness and predicts clinical outcomes better than pulmonary vascular resistance alone in pediatric patients with pulmonary hypertension. Am Heart J. 2008; 155:166–174. [PubMed: 18082509]
57. Hyvelin JM, Howell K, Nichol A, Costello CM, Preston RJ, McLoughlin P. Inhibition of Rho-kinase attenuates hypoxia-induced angiogenesis in the pulmonary circulation. Circ Res. 2005; 97:185–191. [PubMed: 15961717]
58. Ishide N, Shimizu Y, Maruyama Y, Koiwa Y, Nunokawa T, Isoyama S, Kitaoka S, Tamaki K, Ino-Oka E, Takishima T. Effects of changes in the aortic input impedance on systolic pressure-ejected volume relationships in the isolated supported canine left ventricle. Cardiovasc Res. 1980; 14:229–243. [PubMed: 7427971]
59. Jeffery TK, Morrell NW. Molecular and cellular basis of pulmonary vascular remodeling in pulmonary hypertension. Prog Cardiovasc Dis. 2002; 45:173–202. [PubMed: 12525995]
60. Kaebnick BW, Giridharan GA, Koenig SC. Quantification of pulsatility as a function of vascular input impedance: An in vitro study. ASAIO J. 2007; 53:115–121. [PubMed: 17413547]
61. Kass DA. Ventricular arterial stiffening: Integrating the pathophysiology. Hypertension. 2005; 46:185–193. [PubMed: 15911741]
62. Kassab GS, Navia JA. Biomechanical considerations in the design of graft: The homeostasis hypothesis. Annu Rev Biomed Eng. 2006; 8:499–535. [PubMed: 16834565]
63. Klein R, Klein BE, Tomany SC, Cruickshanks KJ. The association of cardiovascular disease with the long-term incidence of age-related maculopathy: The Beaver Dam eye study. Ophthalmology. 2003; 110:636–643. [PubMed: 12689879]
64. Kobs RW, Muvarak NE, Eickhoff JC, Chesler NC. Linked mechanical and biological aspects of remodeling in mouse pulmonary arteries with hypoxia-induced hypertension. Am J Physiol Heart Circ Physiol. 2005; 288:H1209–H1217. [PubMed: 15528223]
65. Kussmaul WG III, Altschuler JA, Herrmann HC, Laskey WK. Effects of pacing tachycardia and balloon valvuloplasty on pulmonary artery impedance and hydraulic power in mitral stenosis. Circulation. 1992; 86:1770–1779. [PubMed: 1451249]
66. Lajemi M, Gautier S, Poirier O, Baguet JP, Mimran A, Gosse P, Hanon O, Labat C, Cambien F, Benetos A. Endothelin gene variants and aortic and cardiac structure in never-treated hypertensives. Am J Hypertens. 2001; 14:755–760. [PubMed: 11497190]
67. Lammers SR, Kao PH, Qi HJ, Hunter K, Lanning C, Albietz J, Hofmeister S, Mecham R, Stenmark KR, Shandas R. Changes in the structure-function relationship of elastin and its impact on the proximal pulmonary arterial mechanics of hypertensive calves. Am J Physiol-Heart C. 2008; 295:H1451–H1459.
68. Launer LJ, Ross GW, Petrovitch H, Masaki K, Foley D, White LR, Havlik RJ. Midlife blood pressure and dementia: The Honolulu-Asia aging study. Neurobiol Aging. 2000; 21:49–55. [PubMed: 10794848]
69. Lavoie TL, Dowell ML, Lakser OJ, Gerthoffer WT, Fredberg JJ, Seow CY, Mitchell RW, Solway J. Disrupting actin-myosin-actin connectivity in airway smoothmuscle as a treatment for asthma? Proc Am Thorac Soc. 2009; 6:295–300. [PubMed: 19387033]

70. Lehoux S, Tedgui A. Cellular mechanics and gene expression in blood vessels. J Biomech. 2003; 36:631–643. [PubMed: 12694993]
71. Li M, Chiou KR, Bugayenko A, Irani K, Kass DA. Reduced wall compliance suppresses Akt-dependent apoptosis protection stimulated by pulse perfusion. Circ Res. 2005; 97:587–595. [PubMed: 16100043]
72. Li M, Scott DE, Shandas R, Stenmark KR, Tan W. High pulsatility flow induces adhesion molecule and cytokine mRNA expression in distal pulmonary artery endothelial cells. Ann Biomed Eng. 2009; 37:1082–1092. [PubMed: 19340571]
73. Li M, Stenmark KR, Shandas R, Tan W. Effects of pathological flow on pulmonary artery endothelial production of vasoactive mediators and growth factors. J Vasc Res. 2009; 46:561–571. [PubMed: 19571576]
74. Lieber, B. Arterial Macrocirculatory Hemodynamics. Bronzino, J., editor. Boca Raton: CRC Press, LLC; 2000.
75. Loutzenhiser R, Bidani A, Chilton L. Renal myogenic response: Kinetic attributes and physiological role. Circ Res. 2002; 90:1316–1324. [PubMed: 12089070]
76. Lucas CL, Wilcox BR, Ha B, Henry GW. Comparison of time domain algorithms for estimating aortic characteristic impedance in humans. IEEE Trans Biomed Eng. 1988; 35:62–68. [PubMed: 3338813]
77. Macchia A, Marchioli R, Marfisi R, Scarano M, Levantesi G, Tavazzi L, Tognoni G. A meta-analysis of trials of pulmonary hypertension: A clinical condition looking for drugs and research methodology. Am Heart J. 2007; 153:1037–1047. [PubMed: 17540207]
78. Mahapatra S, Nishimura RA, Sorajja P, Cha S, McGoon MD. Relationship of pulmonary arterial capacitance and mortality in idiopathic pulmonary arterial hypertension. J Am Coll Cardiol. 2006; 47:799–803. [PubMed: 16487848]
79. Mauban JR, Remillard CV, Yuan JX. Hypoxic pulmonary vasoconstriction: Role of ion channels. J Appl Physiol. 2005; 98:415–420. [PubMed: 15591311]
80. McDonald DA, Taylor MG. The hemodynamics of the arterial circulation. Prog Biophys Chem. 1959; 9:107–173.
81. McDonald, DA. Blood Flow in Arteries. 2nd ed. McDonald, Alison; Nichols, Wilmer W.; Milnor, William R., editors. London: Edward Arnold Ltd.; 1974.
82. Mecham RP, Stenmark KR, Parks WC. Connective tissue production by vascular smooth muscle in development and disease. Chest. 1991; 99:43S–47S. [PubMed: 1997269]
83. Medley TL, Cole TJ, Gatzka CD, Wang WY, Dart AM, Kingwell BA. Fibrillin-1 genotype is associated with aortic stiffness and disease severity in patients with coronary artery disease. Circulation. 2002; 105:810–815. [PubMed: 11854120]
84. Medley TL, Kingwell BA, Gatzka CD, Pillay P, Cole TJ. Matrix metalloproteinase-3 genotype contributes to age-related aortic stiffening through modulation of gene and protein expression. Circ Res. 2003; 92:1254–1261. [PubMed: 12750310]
85. Milnor WR. Arterial impedance as ventricular afterload. Circ Res. 1975; 36:565–570. [PubMed: 1122568]
86. Milnor, WR. Hemodynamics. 2nd ed. Nancy, Collins, editor. Baltimore: Williams & Wilkins; 1989.
87. Milnor WR, Bergel DH, Bargainer JD. Hydraulic power associated with pulmonary blood flow and its relation to heart rate. Circ Res. 1966; 19:467–480. [PubMed: 5925148]
88. Milnor WR, Conti CR, Lewis KB, O'Rourke MF. Pulmonary arterial pulse wave velocity and impedance in man. Circ Res. 1969; 25:637–649. [PubMed: 5364641]
89. Mitchell GF. Increased aortic stiffness: An unfavorable cardiorenal connection. Hypertension. 2004; 43:151–153. [PubMed: 14718350]
90. Mitchell GF. Effects of central arterial aging on the structure and function of the peripheral vasculature: Implications for end-organ damage. J Appl Physiol. 2008; 105:1652–1660. [PubMed: 18772322]
91. Mitchell GF. Arterial stiffness and wave reflection: Biomarkers of cardiovascular risk. Artery Res. 2009a; 3:56–64. [PubMed: 20161241]

92. Mitchell GF. Clinical achievements of impedance analysis. Med Biol Eng Comput. 2009b; 47:153–163. [PubMed: 18853214]

93. Mitchell GF, DeStefano AL, Larson MG, Benjamin EJ, Chen MH, Vasan RS, Vita JA, Levy D. Heritability and a genome-wide linkage scan for arterial stiffness, wave reflection, and mean arterial pressure: The Framingham Heart Study. Circulation. 2005; 112:194–199. [PubMed: 15998672]

94. Mitchell GF, Vita JA, Larson MG, Parise H, Keyes MJ, Warner E, Vasan RS, Levy D, Benjamin EJ. Cross-sectional relations of peripheral microvascular function, cardiovascular disease risk factors, and aortic stiffness: The Framingham Heart Study. Circulation. 2005; 112:3722–3728. [PubMed: 16330686]

95. Morrell NW, Adnot S, Archer SL, Dupuis J, Jones PL, MacLean MR, McMurtry IF, Stenmark KR, Thistlethwaite PA, Weissmann N, Yuan JX, Weir EK. Cellular and molecular basis of pulmonary arterial hypertension. J Am Coll Cardiol. 2009; 54:S20–S31. [PubMed: 19555855]

96. Moudgil R, Michelakis ED, Archer SL. Hypoxic pulmonary vasoconstriction. J Appl Physiol. 2005; 98:390–403. [PubMed: 15591309]

97. Murgo JP, Westerhof N, Giolma JP, Altobelli SA. Aortic input impedance in normal man: Relationship to pressure wave forms. Circulation. 1980; 62:105–116. [PubMed: 7379273]

98. Naeije R, Huez S. Reflections on wave reflections in chronic thromboembolic pulmonary hypertension. Eur Heart J. 2007; 28:785–787. [PubMed: 17384088]

99. Nagaoka T, Fagan KA, Gebb SA, Morris KG, Suzuki T, Shimokawa H, McMurtry IF, Oka M. Inhaled Rho kinase inhibitors are potent and selective vasodilators in rat pulmonary hypertension. Am J Respir Crit Care Med. 2005; 171:494–499. [PubMed: 15563635]

100. Nakayama Y, Nakanishi N, Hayashi T, Nagaya N, Sakamaki F, Satoh N, Ohya H, Kyotani S. Pulmonary artery reflection for differentially diagnosing primary pulmonary hypertension and chronic pulmonary thromboembolism. J Am Coll Cardiol. 2001; 38:214–218. [PubMed: 11451277]

101. Nichols, Wilmer W.; O'Rourke, Michael F. McDonald's Blood Flow in Arteries: Theoretical, Experimental, and Clinical Principles. 5th ed. Joana, Koster, editor. London: A. Hodder Arnold; 1998.

102. Nichols WW, Conti CR, Walker WE, Milnor WR. Input impedance of the systemic circulation in man. Circ Res. 1977; 40:451–458. [PubMed: 856482]

103. Nichols, WW.; O'Rourke, M.; Kenney, W. Mc-Donald's Blood Flow in Arteries: Theoretical, Experimental, and Clinical Principles. 5th ed. Joana, Koster, editor. London: A. Hodder Arnold; 1998. p. 607

104. O'Rourke M. Arterial stiffness, systolic blood pressure, and logical treatment of arterial hypertension. Hypertension. 1990; 15:339–347. [PubMed: 2180816]

105. O'Rourke MF. Vascular impedance in studies of arterial and cardiac function. Physiol Rev. 1982; 62:570–623. [PubMed: 6461866]

106. O'Rourke MF, Mancia G. Arterial stiffness. J Hypertens. 1999; 17:1–4. [PubMed: 10100086]

107. O'Rourke MF, Safar ME. Relationship between aortic stiffening and microvascular disease in brain and kidney: Cause and logic of therapy. Hypertension. 2005; 46:200–204. [PubMed: 15911742]

108. Ooi H, Chung W, Biolo A. Arterial stiffness and vascular load in heart failure. Congest Heart Fail. 2008; 14:31–36. [PubMed: 18256567]

109. Pantoni L, Garcia JH. Cognitive impairment and cellular/vascular changes in the cerebral white matter. Ann N Y Acad Sci. 1997; 826:92–102. [PubMed: 9329683]

110. Pauca AL, O'Rourke MF, Kon ND. Prospective evaluation of a method for estimating ascending aortic pressure from the radial artery pressure waveform. Hypertension. 2001; 38:932–937. [PubMed: 11641312]

111. Pauca AL, Wallenhaupt SL, Kon ND, Tucker WY. Does radial artery pressure accurately reflect aortic pressure? Chest. 1992; 102:1193–1198. [PubMed: 1395767]

112. Peled N, Shitrit D, Fox BD, Shlomi D, Amital A, Bendayan D, Kramer MR. Peripheral arterial stiffness and endothelial dysfunction in idiopathic and scleroderma associated pulmonary arterial hypertension. J Rheumatol. 2009; 36:970–975. [PubMed: 19369472]

113. Peng X, Haldar S, Deshpande S, Irani K, Kass DA. Wall stiffness suppresses Akt/eNOS and cytoprotection in pulse-perfused endothelium. Hypertension. 2003; 41:378–381. [PubMed: 12574111]
114. Pepine CJ, Nichols WW, Conti CR. Aortic input impedance in heart failure. Circulation. 1978; 58:460–465. [PubMed: 679436]
115. Piene H. Impedance matching between ventricle and load. Ann Biomed Eng. 1984; 12:191–207. [PubMed: 6507966]
116. Piene H. Pulmonary arterial impedance and right ventricular function. Physiol Rev. 1986; 66:606–652. [PubMed: 3526365]
117. Piene H, Sund T. Does normal pulmonary impedance constitute the optimum load for the right ventricle? Am J Physiol. 1982; 242:H154–H160. [PubMed: 7065148]
118. Qiu H, Zhu Y, Sun Z, Trzeciakowski JP, Gansner M, Depre C, Resuello RR, Natividad FF, Hunter WC, Genin GM, Elson EL, Vatner DE, Meininger GA, Vatner SF. Short communication: Vascular smooth muscle cell stiffness as a mechanism for increased aortic stiffness with aging. Circ Res. 107:615–619. [PubMed: 20634486]
119. Reeves JT, Groves BM, Turkevich D. The case for treatment of selected patients with primary pulmonary hypertension. Am Rev Respir Dis. 1986; 134:342–346. [PubMed: 3740659]
120. Remillard CV, Yuan JX. High altitude pulmonary hypertension: Role of K+ and Ca2+ channels. High Alt Med Biol. 2005; 6:133–146. [PubMed: 16060848]
121. Rodes-Cabau J, Domingo E, Roman A, Majo J, Lara B, Padilla F, Anivarro I, Angel J, Tardif JC, Soler-Soler J. Intravascular ultrasound of the elastic pulmonary arteries: A new approach for the evaluation of primary pulmonary hypertension. Heart. 2003; 89:311–315. [PubMed: 12591838]
122. Safar, M. Arterial Stiffness in Hypertension. Safar, M.; O'Rourke, M., editors. Edinburgh: Elsevier; 2006.
123. Safar ME. Systolic blood pressure, pulse pressure and arterial stiffness as cardiovascular risk factors. Curr Opin Nephrol Hypertens. 2001; 10:257–261. [PubMed: 11224702]
124. Safar ME. Pulse pressure, arterial stiffness and wave reflections (augmentation index) as cardiovascular risk factors in hypertension. Ther Adv Cardiovasc Dis. 2008; 2:13–24. [PubMed: 19124404]
125. Safar ME, London GM, Plante GE. Arterial stiffness and kidney function. Hypertension. 2004; 43:163–168. [PubMed: 14732732]
126. Safar ME, Struijker-Boudier HA. Cross-talk between macro- and microcirculation. Acta Physiol (Oxf). 2010; 198:417–430. [PubMed: 20050837]
127. Safar ME, Thuilliez C, Richard V, Benetos A. Pressure-independent contribution of sodium to large artery structure and function in hypertension. Cardiovasc Res. 2000; 46:269–276. [PubMed: 10773231]
128. Sanz J, Kariisa M, Dellegrottaglie S, Prat-Gonzalez S, Garcia MJ, Fuster V, Rajagopalan S. Evaluation of pulmonary artery stiffness in pulmonary hypertension with cardiac magnetic resonance. JACC Cardiovasc Imaging. 2009; 2:286–295. [PubMed: 19356573]
129. Saouti N, Westerhof N, Helderman F, Marcus JT, Boonstra A, Postmus PE, Vonk Noordegraaf A. Right ventricular oscillatory power is a constant fraction of total power irrespective of pulmonary artery pressure. Am J Respir Crit Care Med. 2010; 182:1315–1320. [PubMed: 20622041]
130. Sokolis DP, Kefaloyannis EM, Kouloukoussa M, Marinos E, Boudoulas H, Karayannacos PE. A structural basis for the aortic stress-strain relation in uniaxial tension. J Biomech. 2006; 39:1651–1662. [PubMed: 16045914]
131. Stenmark KR, Davie N, Frid M, Gerasimovskaya E, Das M. Role of the adventitia in pulmonary vascular remodeling. Physiology (Bethesda). 2006; 21:134–145. [PubMed: 16565479]
132. Stenmark KR, Fagan KA, Frid MG. Hypoxia-induced pulmonary vascular remodeling: Cellular and molecular mechanisms. Circ Res. 2006; 99:675–691. [PubMed: 17008597]
133. Stenmark KR, McMurtry IF. Vascular remodeling versus vasoconstriction in chronic hypoxic pulmonary hypertension: A time for reappraisal? Circ Res. 2005; 97:95–98. [PubMed: 16037575]
134. Stenmark KR, Mecham RP. Cellular and molecular mechanisms of pulmonary vascular remodeling. Annu Rev Physiol. 1997; 59:89–144. [PubMed: 9074758]

135. Streeter VL, Keitzer WF, Bohr DF. Pulsatile pressure and flow through distensible vessels. Circ Res. 1963; 13:3–20. [PubMed: 14042827]
136. Suga H, Kitabatake A, Sagawa K. End-systolic pressure determines stroke volume from fixed end-diastolic volume in the isolated canine left ventricle under a constant contractile state. Circ Res. 1979; 44:238–249. [PubMed: 761306]
137. Sunagawa K, Maughan WL, Burkhoff D, Sagawa K. Left ventricular interaction with arterial load studied in isolated canine ventricle. Am J Physiol. 1983; 245:H773–H780. [PubMed: 6638199]
138. Tagawa H. Pulmonary arterial input impedance in patients with chronic pulmonary diseases. Nihon Kyobu Shikkan Gakkai Zasshi. 1989; 27:1031–1039. [PubMed: 2585900]
139. Taylor MG. Wave-travel in a non-uniform transmission line, in relation to pulses in arteries. Phys Med Biol. 1965; 10:539–550.
140. Tobise K, Haneda T, Onodera S. Changes in the pulmonary vascular input impedance in patients with atrial septal defect after surgical correction. Jpn Circ J. 1990; 54:175–182. [PubMed: 2355451]
141. Travis AR, Giridharan GA, Pantalos GM, Dowling RD, Prabhu SD, Slaughter MS, Sobieski M, Undar A, Farrar DJ, Koenig SC. Vascular pulsatility in patients with a pulsatile- or continuous-flow ventricular assist device. J Thorac Cardiovasc Surg. 2007; 133:517–524. [PubMed: 17258591]
142. Tuder RM, Abman SH, Braun T, Capron F, Stevens T, Thistlethwaite PA, Haworth SG. Development and pathology of pulmonary hypertension. J Am Coll Cardiol. 2009; 54:S3–S9. [PubMed: 19555856]
143. Tuder RM, Marecki JC, Richter A, Fijalkowska I, Flores S. Pathology of pulmonary hypertension. Clin Chest Med. 2007; 28:23–42. [PubMed: 17338926]
144. Undar A, Zapanta CM, Reibson JD, Souba M, Lukic B, Weiss WJ, Snyder AJ, Kunselman AR, Pierce WS, Rosenberg G, Myers JL. Precise quantification of pressure flow waveforms of a pulsatile ventricular assist device. ASAIO J. 2005; 51:56–59. [PubMed: 15745135]
145. Uren NG, Oakley CM. The treatment of primary pulmonary hypertension. Br Heart J. 1991; 66:119–121. [PubMed: 1883661]
146. Vermeer SE, Prins ND, den Heijer T, Hofman A, Koudstaal PJ, Breteler MM. Silent brain infarcts and the risk of dementia and cognitive decline. N Engl J Med. 2003; 348:1215–1222. [PubMed: 12660385]
147. Vernooij MW, van der Lugt A, Ikram MA, Wielopolski PA, Niessen WJ, Hofman A, Krestin GP, Breteler MM. Prevalence and risk factors of cerebral microbleeds: The Rotterdam Scan Study. Neurology. 2008; 70:1208–1214. [PubMed: 18378884]
148. Veyssier-Belot C, Cacoub P. Role of endothelial and smooth muscle cells in the physiopathology and treatment management of pulmonary hypertension. Cardiovasc Res. 1999; 44:274–282. [PubMed: 10690304]
149. Waldstein SR, Rice SC, Thayer JF, Najjar SS, Scuteri A, Zonderman AB. Pulse pressure and pulse wave velocity are related to cognitive decline in the Baltimore Longitudinal Study of Aging. Hypertension. 2008; 51:99–104. [PubMed: 18025297]
150. Weinberg CE, Hertzberg JR, Ivy DD, Kirby KS, Chan KC, Valdes-Cruz L, Shandas R. Extraction of pulmonary vascular compliance, pulmonary vascular resistance, and right ventricular work from single-pressure and Doppler flow measurements in children with pulmonary hypertension: A new method for evaluating reactivity: In vitro and clinical studies. Circulation. 2004; 110:2609–2617. [PubMed: 15492299]
151. Willum-Hansen T, Staessen JA, Torp-Pedersen C, Rasmussen S, Thijs L, Ibsen H, Jeppesen J. Prognostic value of aortic pulse wave velocity as index of arterial stiffness in the general population. Circulation. 2006; 113:664–670. [PubMed: 16461839]
152. Wohrley JD, Frid MG, Moiseeva EP, Orton EC, Belknap JK, Stenmark KR. Hypoxia selectively induces proliferation in a specific subpopulation of smooth muscle cells in the bovine neonatal pulmonary arterial media. J Clin Invest. 1995; 96:273–281. [PubMed: 7615796]
153. Wolinsky H, Glagov S. Structural basis for the static mechanical properties of the aortic media. Circulation Research. 1964; 14:400. [PubMed: 14156860]

154. Wuyts F, Vanhuyse V, Langewouters G, Decraemer W, Raman E, Buyle S. Elastic properties of human aortas in relation to age and atherosclerosis: A structural model. Phys Med Biol. 1995; 40:1577–1597. [PubMed: 8532741]

155. Yin FC, Weisfeldt ML, Milnor WR. Role of aortic input impedance in the decreased cardiovascular response to exercise with aging in dogs. J Clin Invest. 1981; 68:28–38. [PubMed: 7251864]

156. Zhang YH, Dunn ML, Drexler ES, McCowan CN, Slifka AJ, Ivy DD, Shandas R. A microstructural hyperelastic model of pulmonary arteries under normo- and hypertensive conditions. Ann Biomed Eng. 2005; 33:1042–1052. [PubMed: 16133913]

157. Zieman SJ, Melenovsky V, Clattenburg L, Corretti MC, Capriotti A, Gerstenblith G, Kass DA. Advanced glycation endproduct crosslink breaker (alagebrium) improves endothelial function in patients with isolated systolic hypertension. J Hypertens. 2007; 25:577–583. [PubMed: 17278974]

158. Zuckerman BD, Orton EC, Latham LP, Barbiere CC, Stenmark KR, Reeves JT. Pulmonary vascular impedance and wave reflections in the hypoxic calf. J Appl Physiol. 1992; 72:2118–2127. [PubMed: 1629064]

159. Zuckerman BD, Orton EC, Stenmark KR, Trapp JA, Murphy JR, Coffeen PR, Reeves JT. Alteration of the pulsatile load in the high-altitude calf model of pulmonary hypertension. J Appl Physiol. 1991; 70:859–868. [PubMed: 2022578]

160. Zulliger MA, Rachev A, Stergiopulos N. A constitutive formulation of arterial mechanics including vascular smooth muscle tone. Am J Physiol Heart Circ Physiol. 2004; 287:H1335–H1343. [PubMed: 15130890]

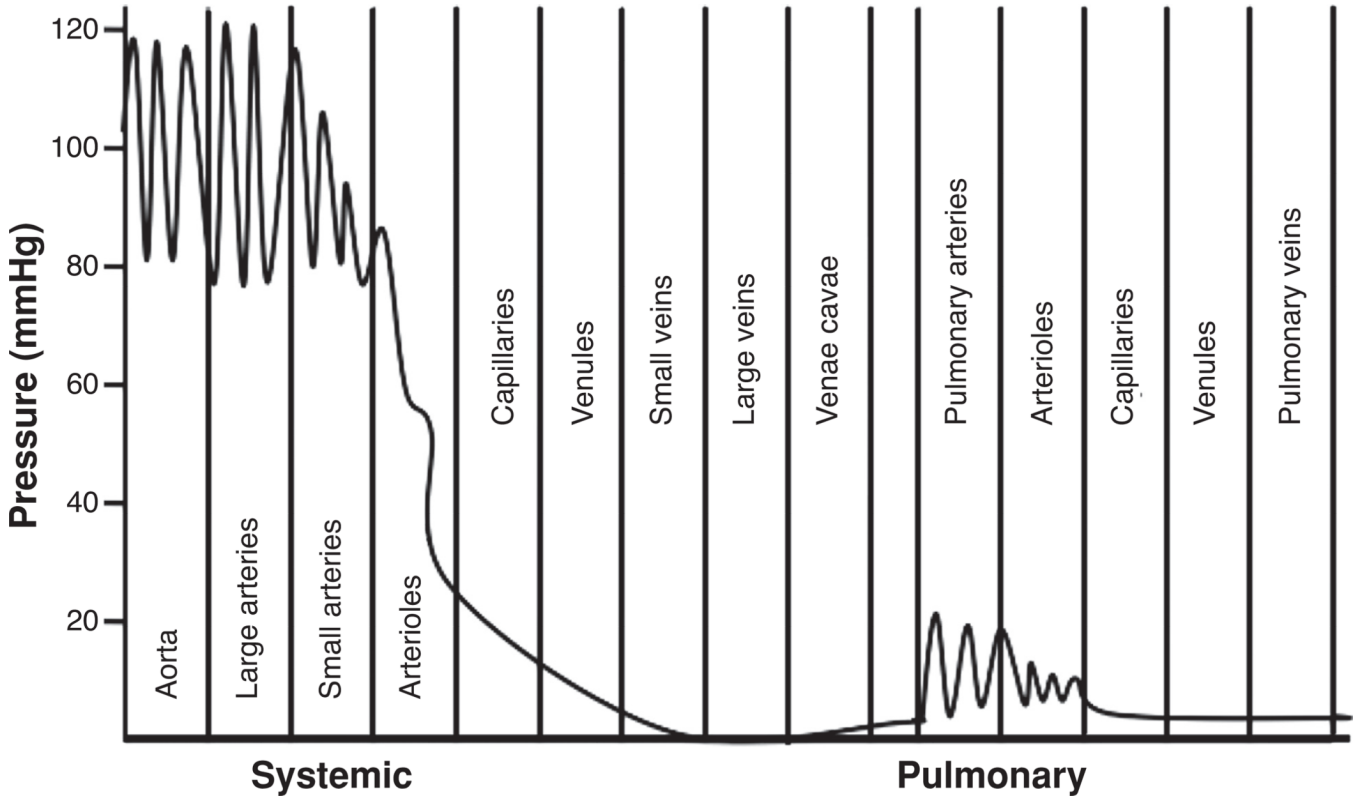

Figure 1.
Normal blood pressures of the systemic and pulmonary circulatory systems. Pulmonary circulation has much lower pressures and pulsations extend into the capillaries. (Redrawn, with permission, by Devon Scott.)

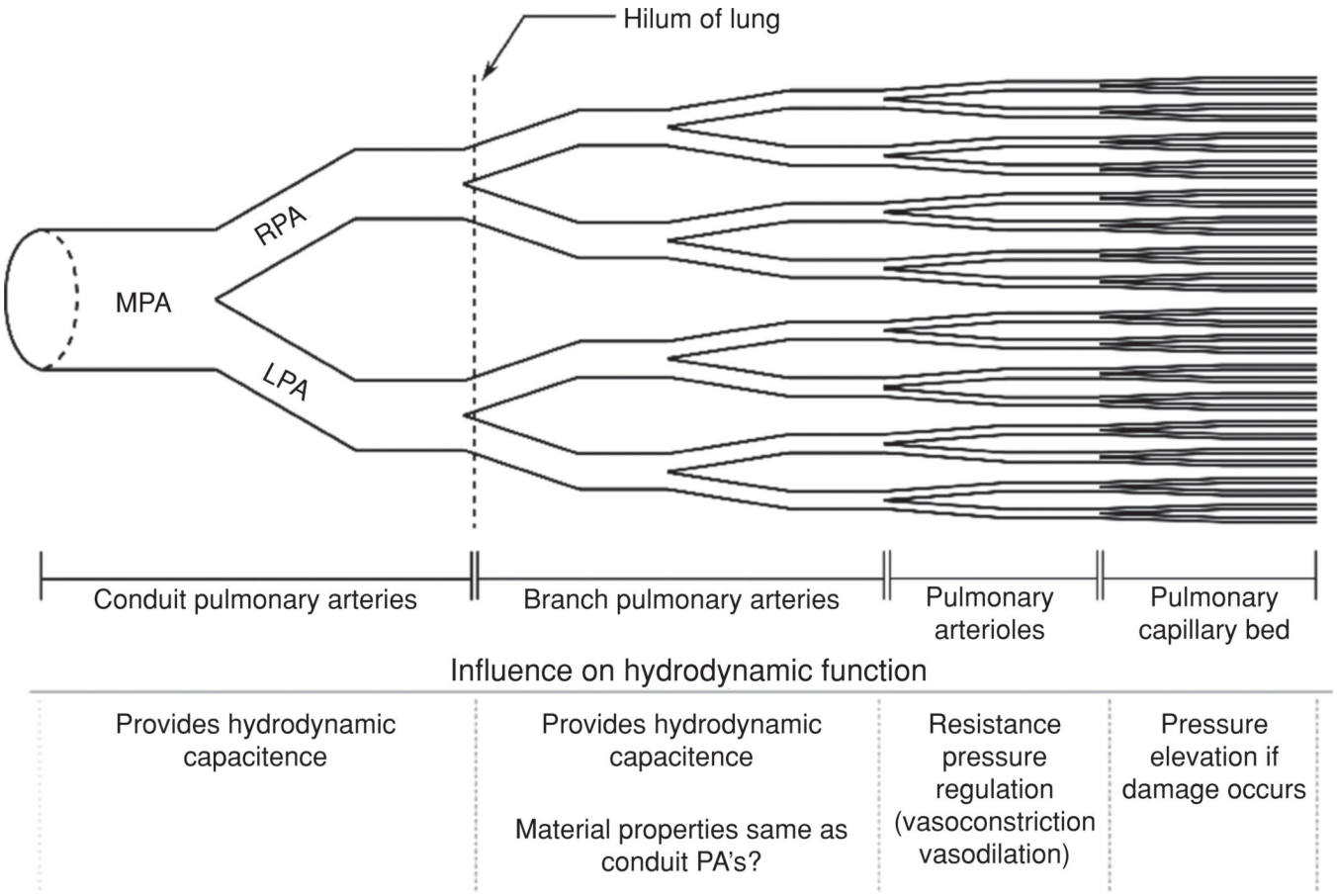

Figure 2.
Diagram of pulmonary vascular tree.

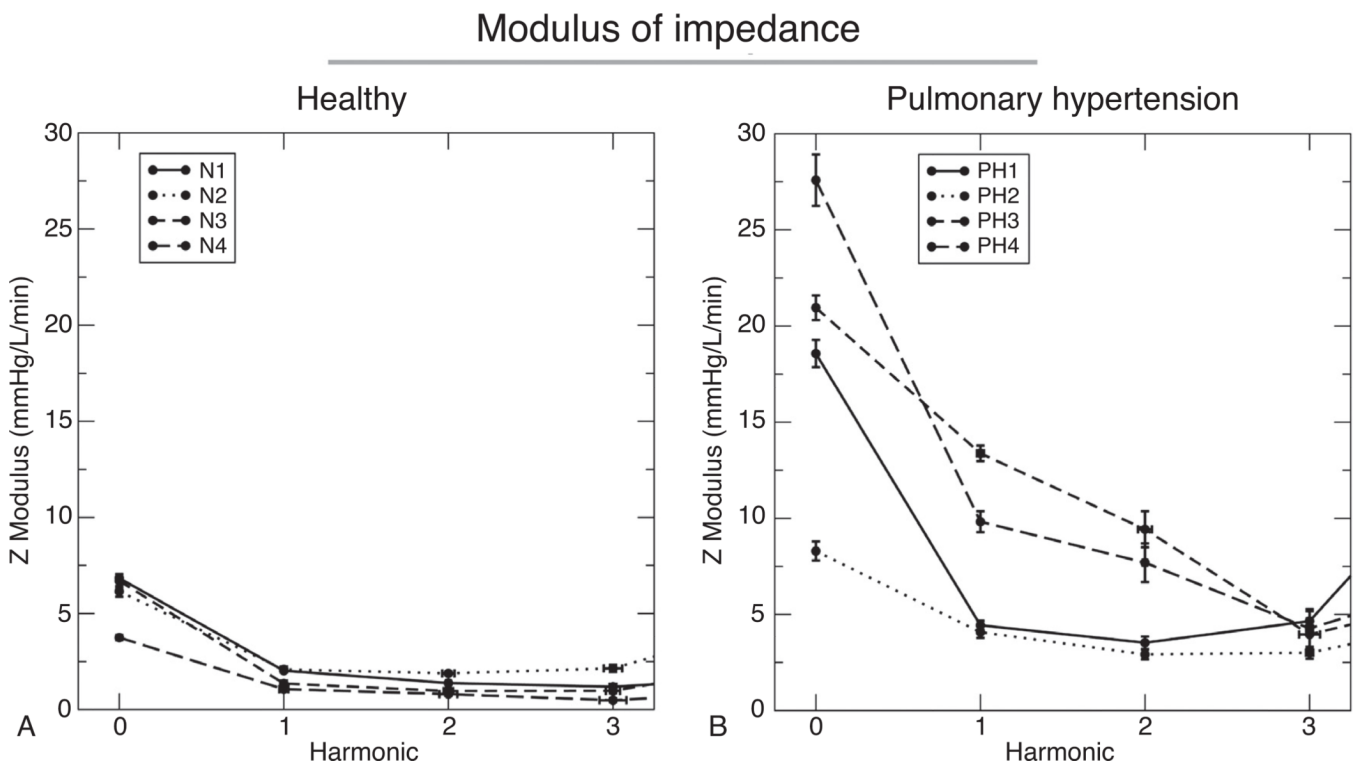

Figure 3.

Impedance modulus in healthy (A) and pulmonary hypertensive (B) children. As with other clinical studies of impedance, pulmonary hypertensive individuals displayed both larger values of Z_0, corresponding to higher PVR and larger values of the first several harmonics of impedance. Further, the first minimum of the curve is shifted rightward in the PH patients, corresponding to higher pulse-wave velocities (56).

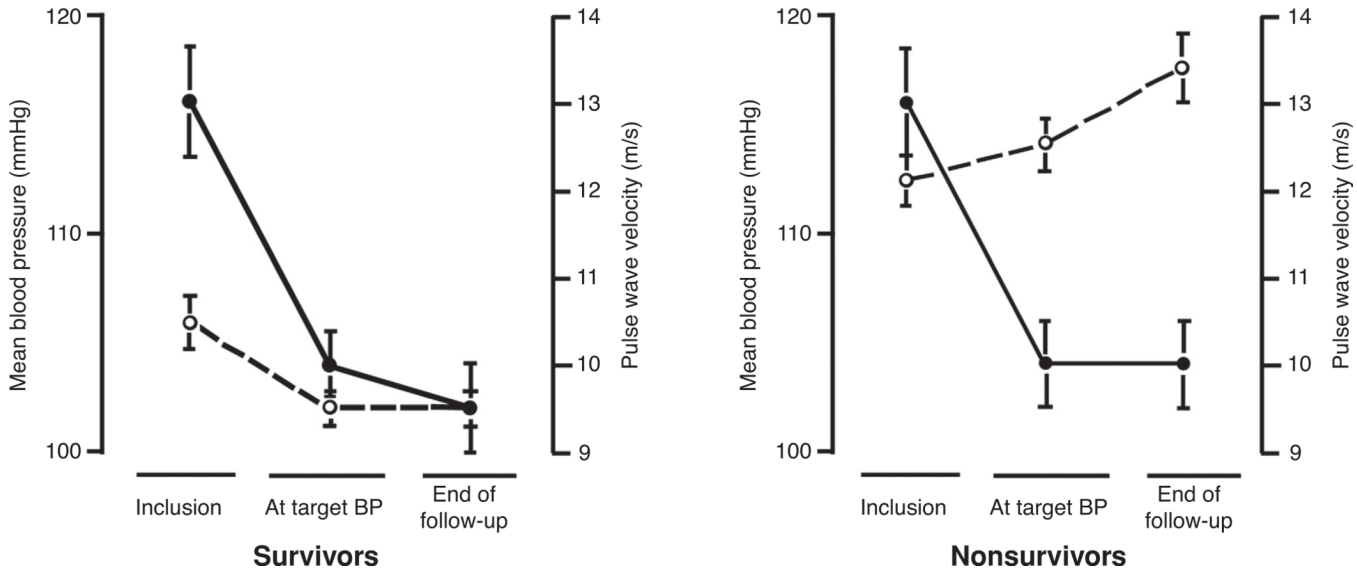

Figure 4.

Changes in mean blood pressure (MBP) (solid circle) and aortic pulse wave velocity (PWV) (open circle) for survivors and nonsurvivors of systemic hypertension in end-stage renal disease. Patients underwent antihypertensive therapy and were tracked from inclusion to end of follow-up (45).

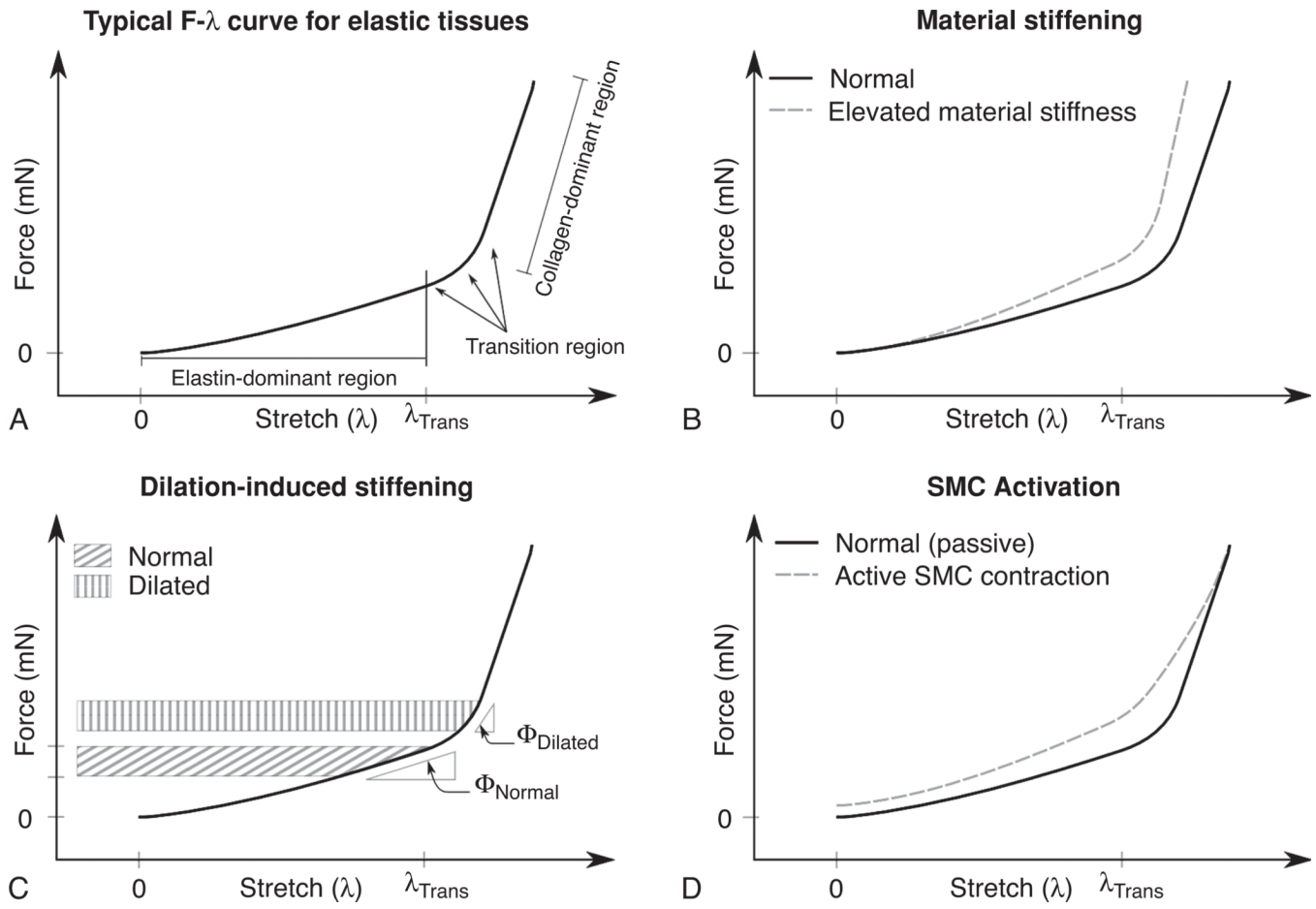

Figure 5.
Mechanisms of arterial stiffening. Panels A, B, C, and D are discussed in detail in the text.

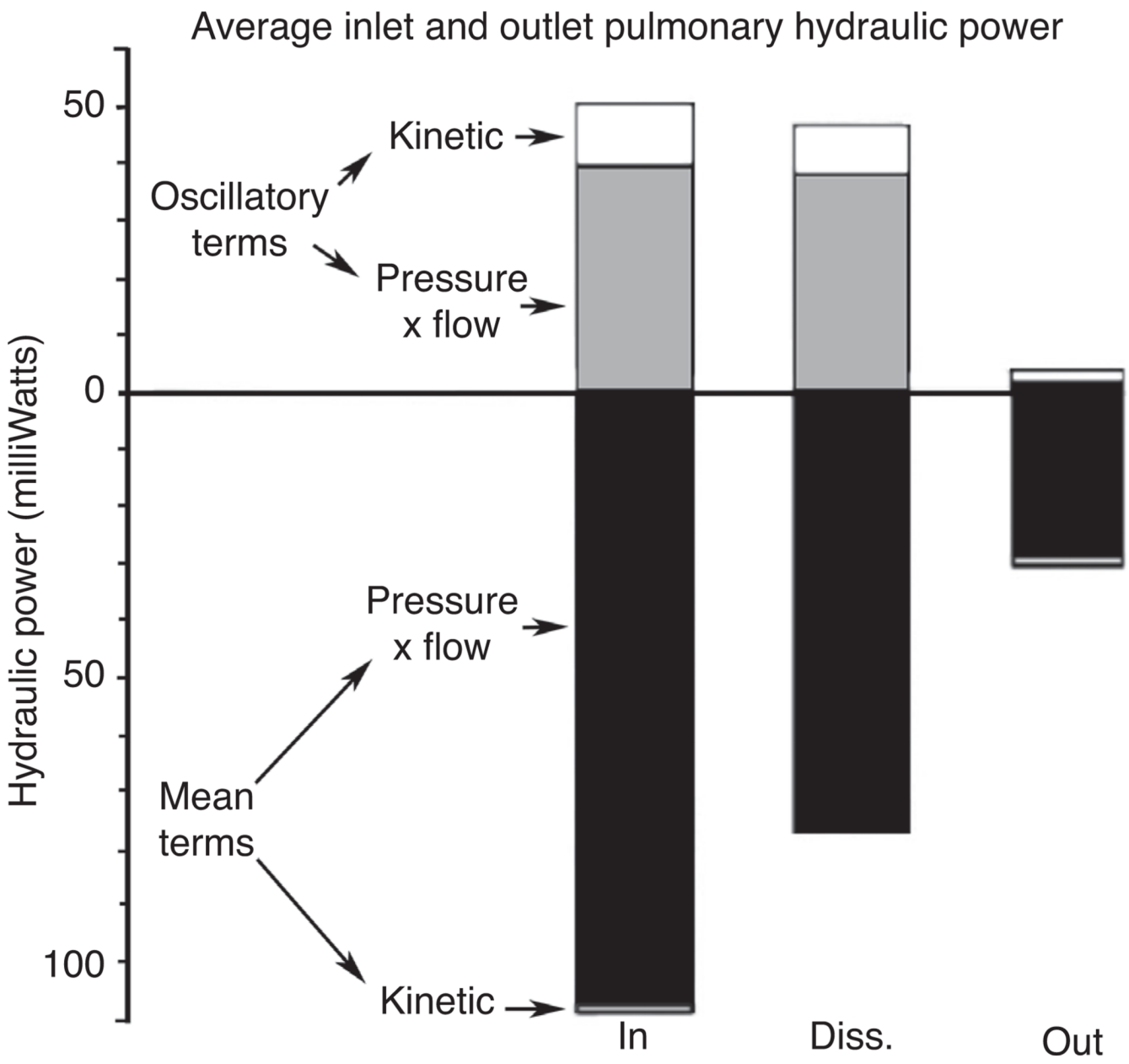

Figure 6.

Average hydraulic power of the inlet (IN, MPA) and outlet (OUT, pulmonary vein, near left atrium) of the pulmonary bed of anesthetized, open-chest dogs. Regions above and below the hydraulic power = 0 line are both positive valued. Upper region contains pressure-potential and kinetic energy terms associated with oscillatory component of blood flow. Lower region contains analogous terms for the steady-flow component. Input and output hydraulic power values are shown in their respective columns with the difference between the two being the power dissipated (DISS) throughout the pulmonary bed during the cardiac cycle (87).

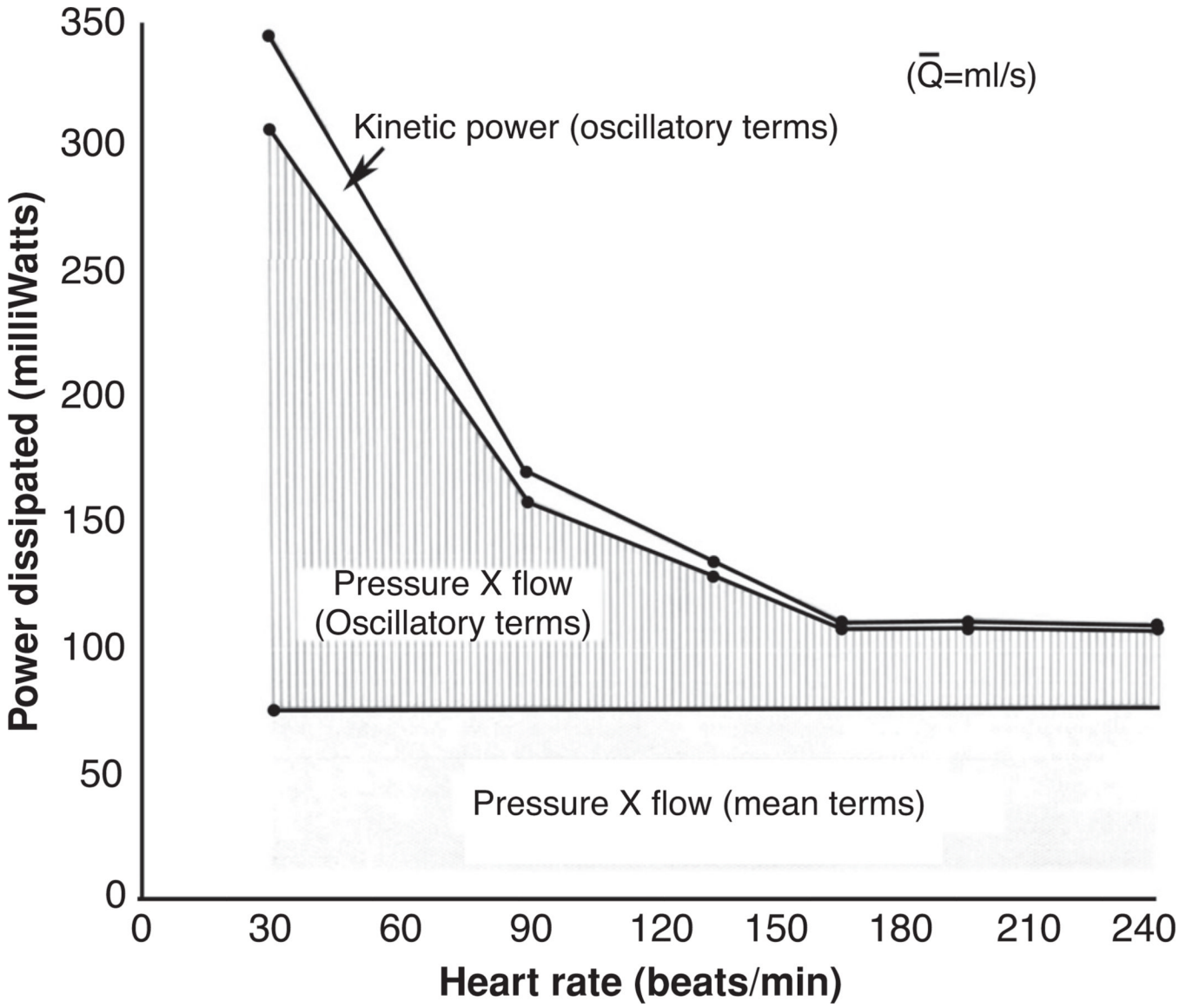

Figure 7.
Power dissipated as a function of heart rate for a constant pulmonary flow of 42.0 cm^3/s measured in anesthetized dogs (87).

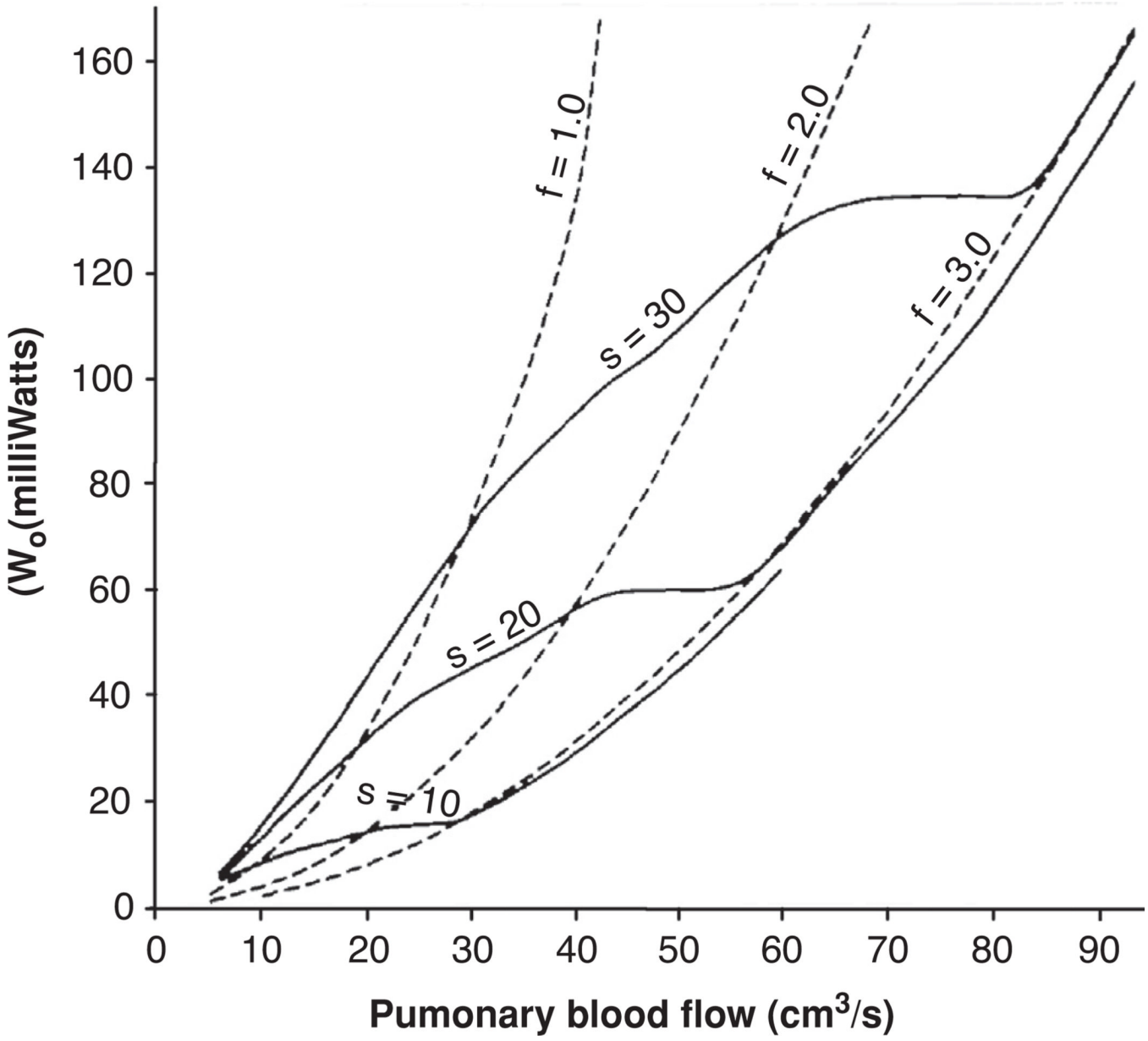

Figure 8.

Oscillatory component of input power (ordinate) at different levels of pulmonary blood flow (abscissa) for three different heart rates at constant stroke volume (solid line) and for three different stroke volumes at constant heart rate (solid line). Constant stroke volume curves are shown for three volumes (S = 10, 20, and 30 cm^3/stroke) and constant heart rate curves are shown for three rates (f = 1.0, 2.0, and 3.0 beats/s). Constant stroke volume and constant heart rate curves are nearly equal for heart rates above 3 beats/s. Plot shows that pulmonary blood flow can be increased more efficiently by increasing heart rate than by increasing stroke volume (87).

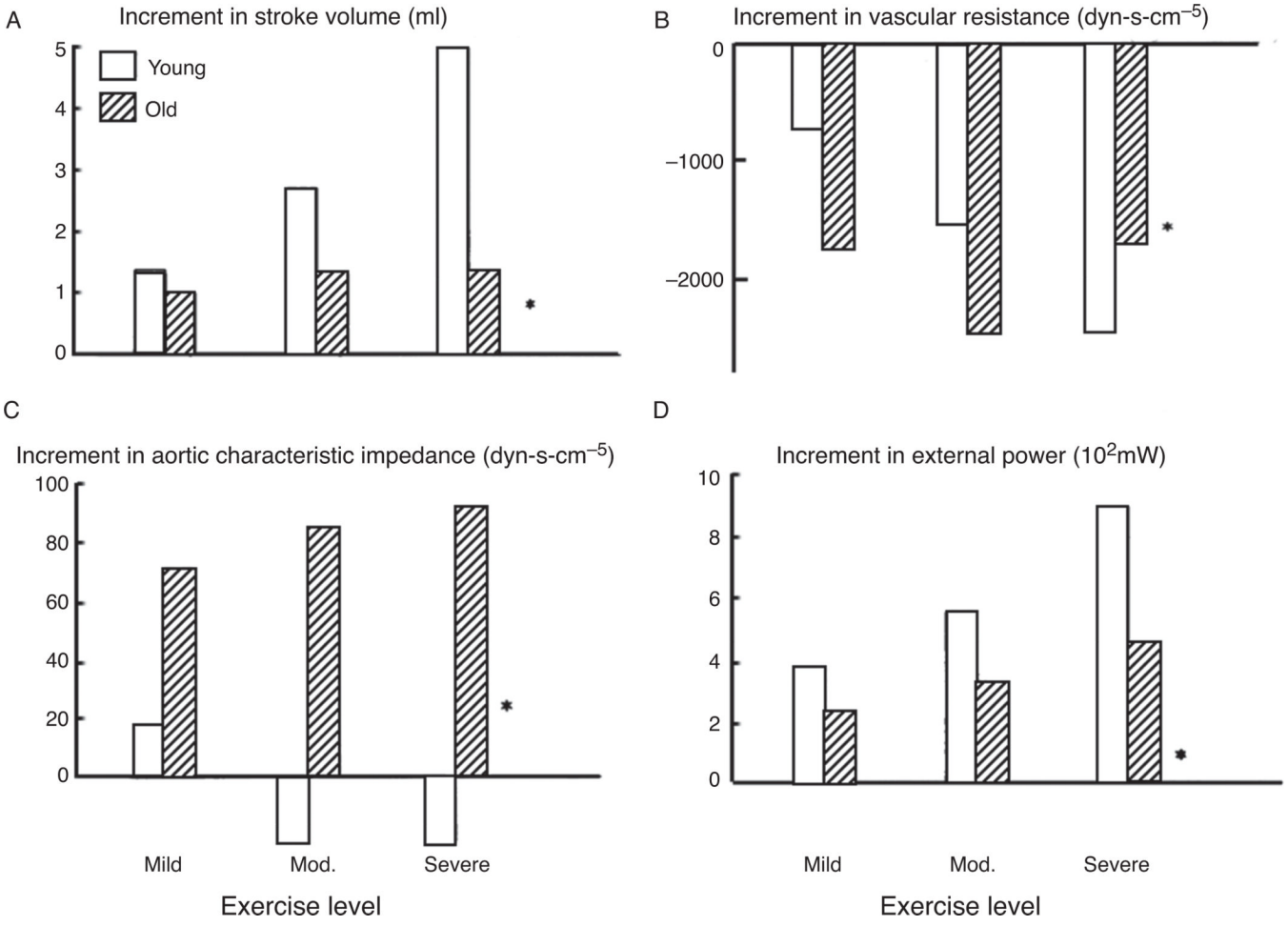

Figure 9.

Effect of graded exercise on the increment in stroke volume (A), vascular resistance (B), aortic characteristic impedance (C), and external power (D) represented as mean change from resting values for young and old dogs at three different levels of exercise, $*P = 0.05$ (between young and old) (155).

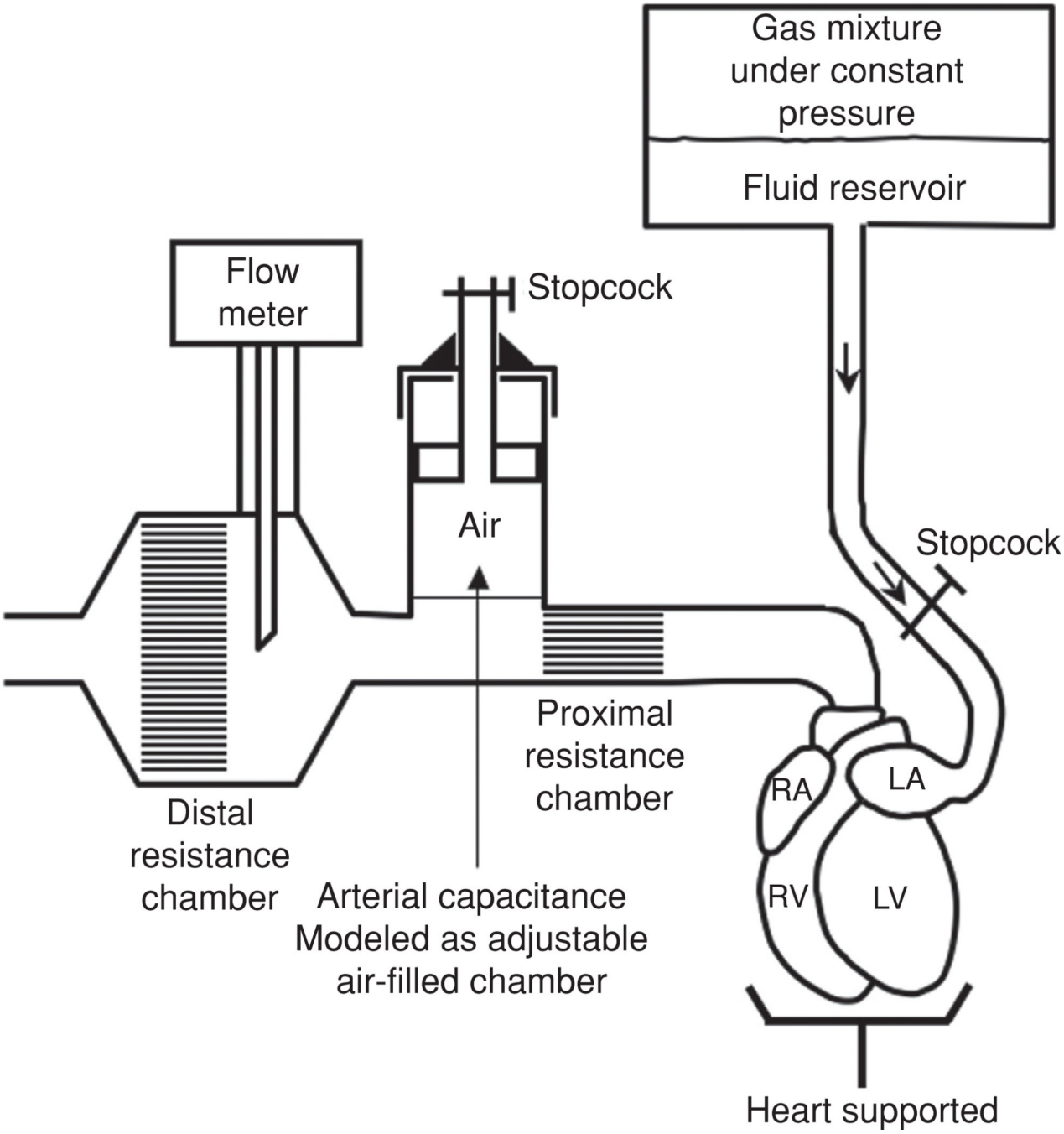

Figure 10.
Schematic of pressure-controlled isolated supported ventricle (PCISV). *R*, central reservoir; C2, C3, and C4, stopcocks; SL, supply container; OL, overflow system; RL, small reservoir; RP peripheral resistance; F, filter; RC characteristic impedance; and C capacitance (33).

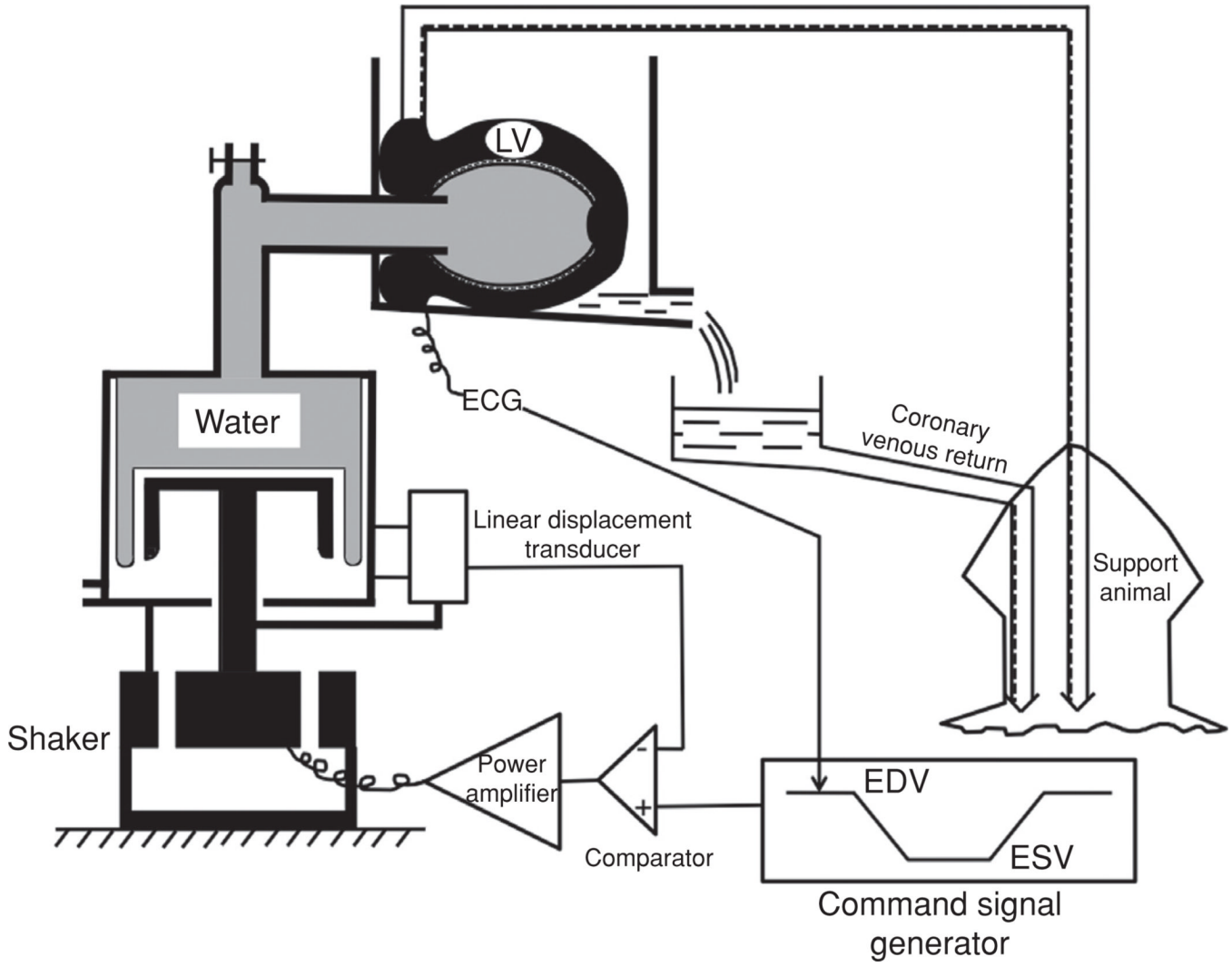

Figure 11.
Schematic of volume controlled isolated supported ventricle (VCISV). A, coronary perfusion tube; AV, air vent; B, sealed box in which heart was placed for testing; BC, Bellofram cylinder; C, comparator; E, error signal; EDV, end diastolic volume; ESV, end systolic volume; HE, heat exchanger; LT, linear displacement transducer; LV, left ventricle; NP, negative pressure applied behind the diaphragm to reduce the compliance of the rolling diaphragm; PA, power amplifier; V, coronary venous return tube; VP, ventricular pressure measured by a miniature gage; VV, ventricular volume signal; W, hydraulic fluid (water) (136).

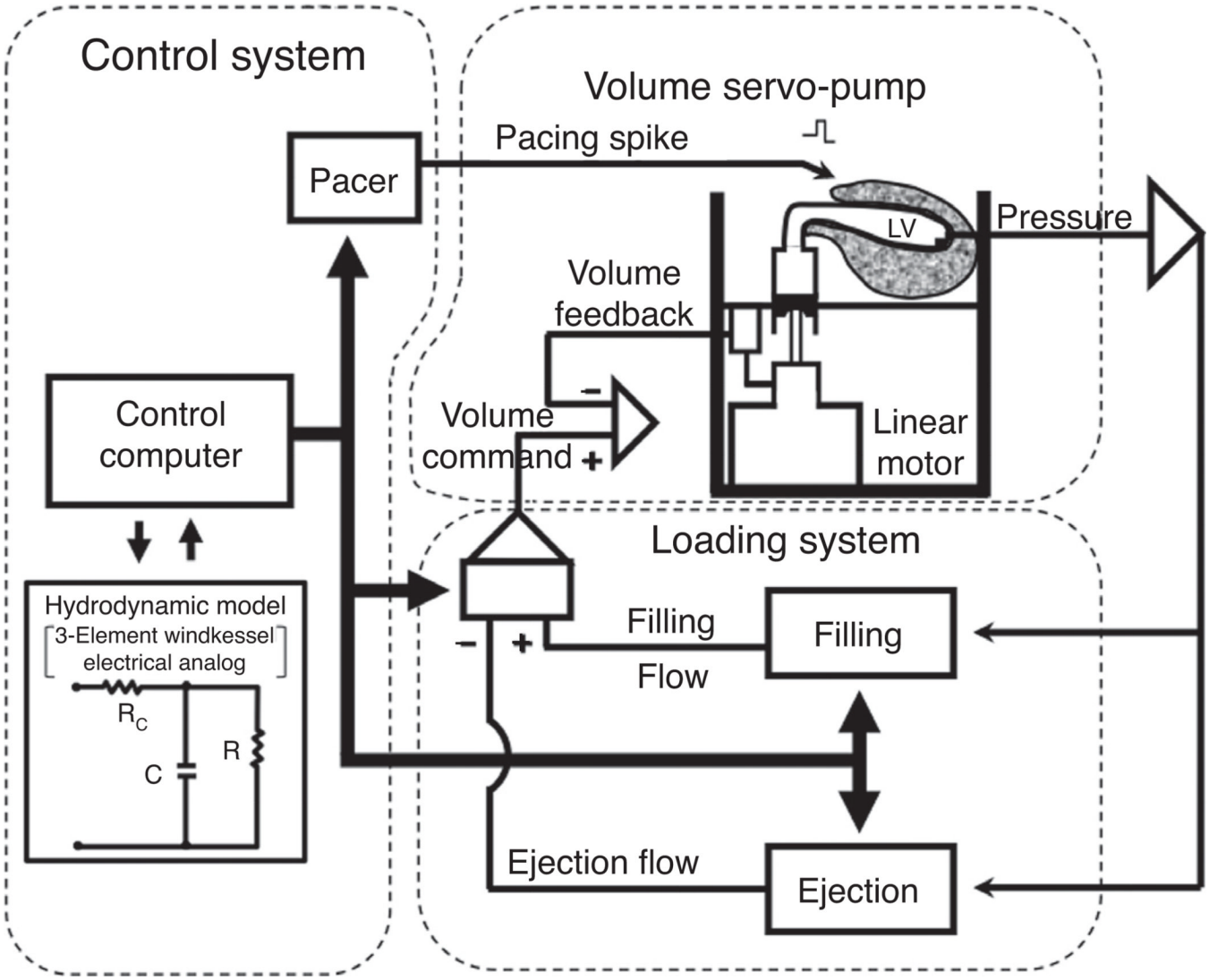

Figure 12.
Diagram of the Windkessel controlled isolated supported ventricle (WCISV). A linear motor and piston-pump assembly allows for precise control of instantaneous ventricular volume. Loading system computes instantaneous ventricular pressure-flow data in real time. Control system imposed real time pressure flow relationship based on three-element Windkessel model through control of the linear motor (137).

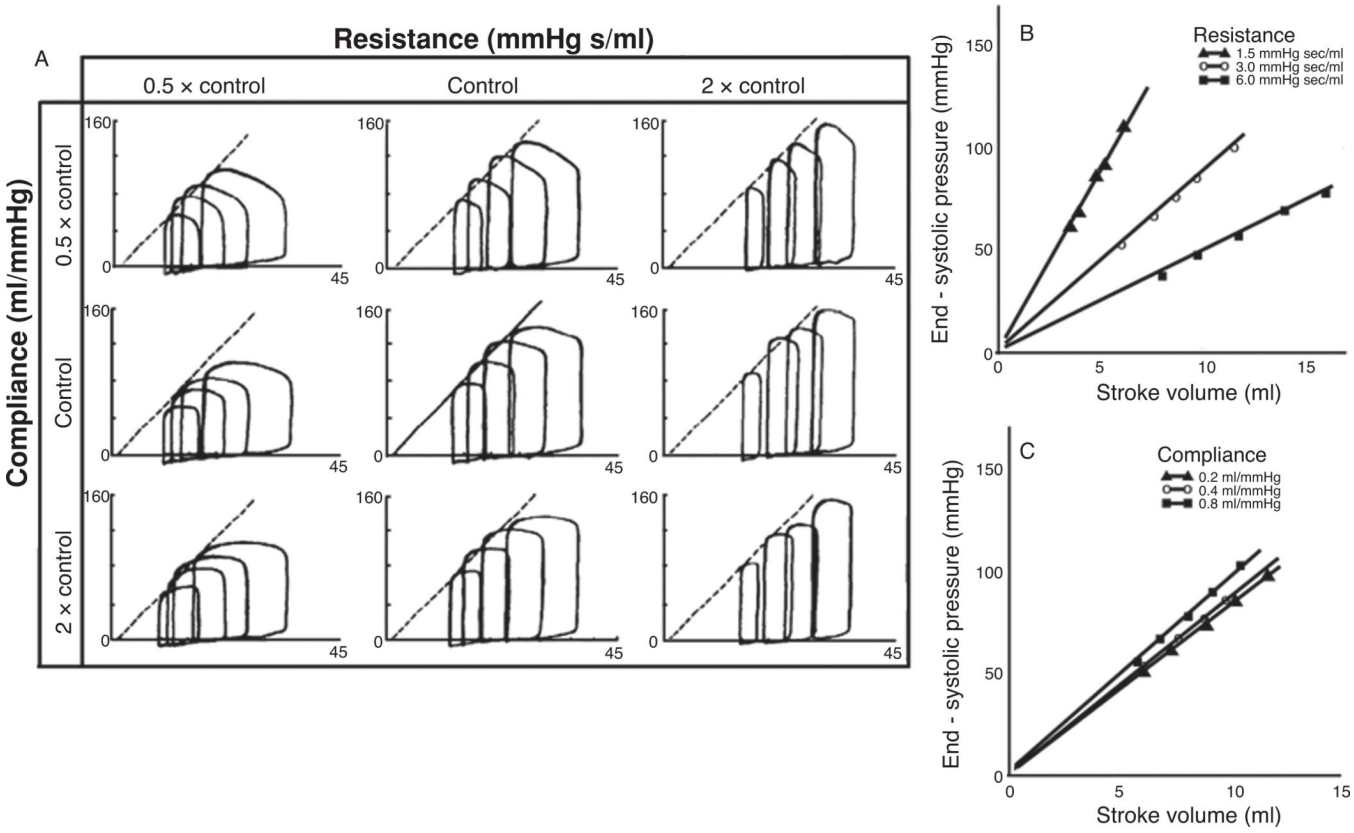

Figure 13.

Example of typical Windkessel controlled isolated supported ventricle (WCISV) dataset. Experimental protocol consisted of first determining control values for the distal vascular resistance, characteristic impedance, and arterial compliance of the normal animal; which were 3.0 mmHg-s/ml, 0.2 mmHg-s/ml, and 0.4 ml/mmHg, respectively, for dogs weighing 20 to 22 kg. Arterial compliance and resistance were varied by 50% and 200% of control values while *P-V* loops were generated at four end-diastolic volumes for each experimental condition. Characteristic impedance was kept at control value. Heart rate was kept constant during all experiments (127 ± 9 beats/min) by pacing. Solid line at control indicates *P-V* relationship at control conditions, dashed lines in other panels indicate transcribed *P-V* relationship line from control. (B) and (C) End-systolic pressure versus stroke with varying resistance and capacitance, symbols represent experimental data (137).

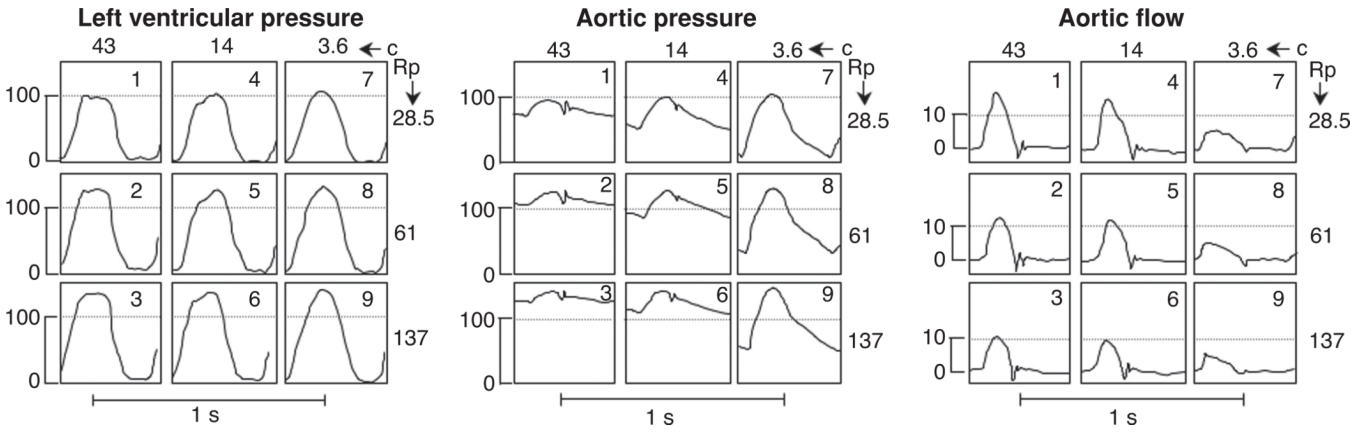

Figure 14.

pressure-controlled isolated supported ventricle (PCISV) model showing the effect that changes in resistance and compliance have on the left ventricular pressure, aortic pressure, and aortic flow measured from cat left ventricle. Distal resistance was increased from a control value of 28.5 g/(cm^{4}s) to 61 and 137 g/(cm^{4}s). Aortic compliance was decreased from a control value of 43 cm^{4}s^2/g to 14 and 3.6 cm^{4}s^2/g. Heart rate was maintained constant at 153 beats/min by pacing. Results from this model for aggregated data from six feline PCISV hearts exposed to a 208% increase in resistance and a 21% decrease in compliance are given in Table 3. Similar results were obtained for changes in the resistance and compliance parameters of PCISV hearts from dogs (33).

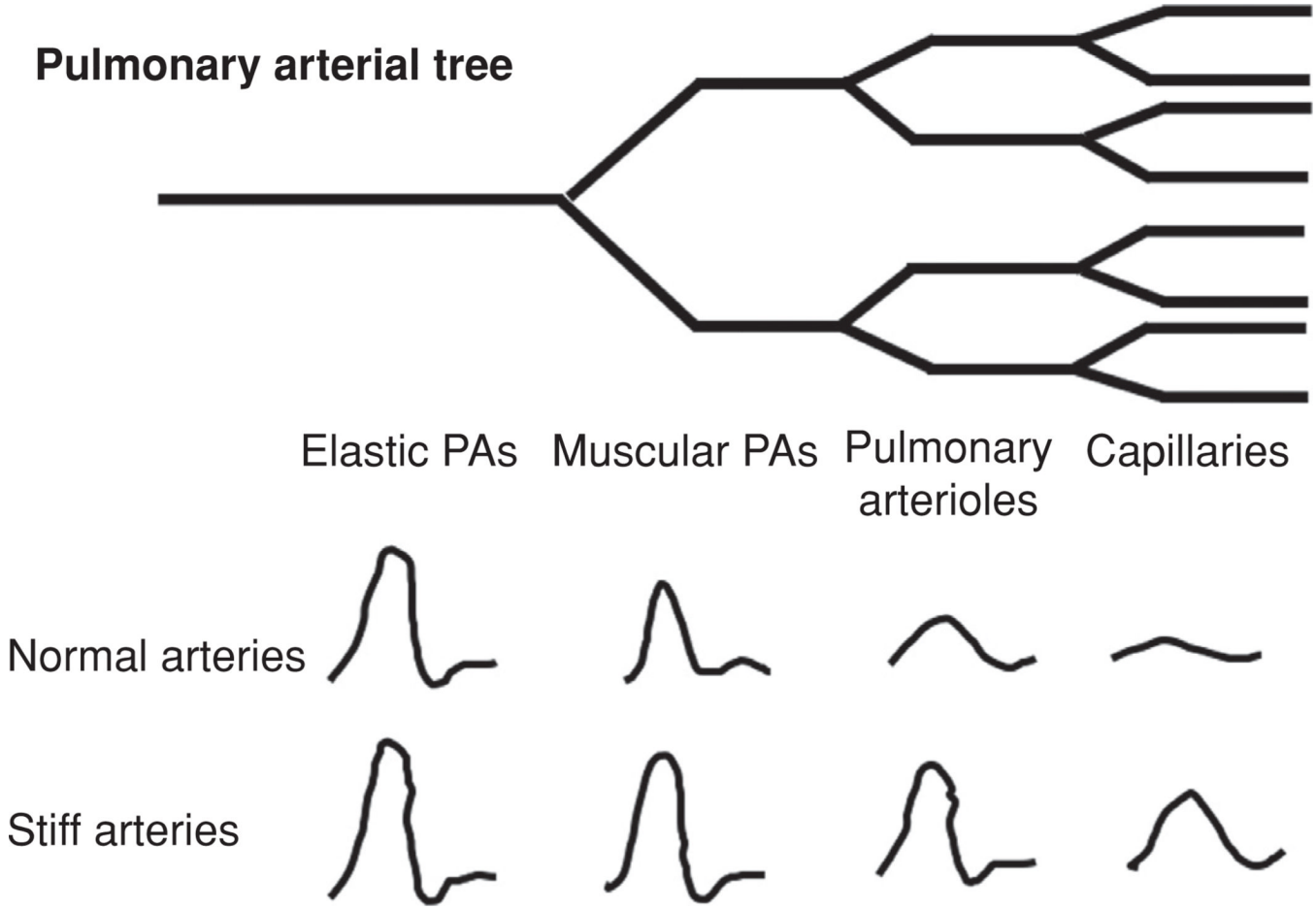

Figure 15.

The experimental approach was to increase the distal resistance from a control value of 28.5 g/(cm^{4}s) to 61 and 137 g/(cm^{4}s) and to decrease the aortic compliance from a control value of 43 cm^{4}s^2/g to 14 and 3.6 cm^{4}s^2/g while maintaining a constant heart rate of 153 beats/min.

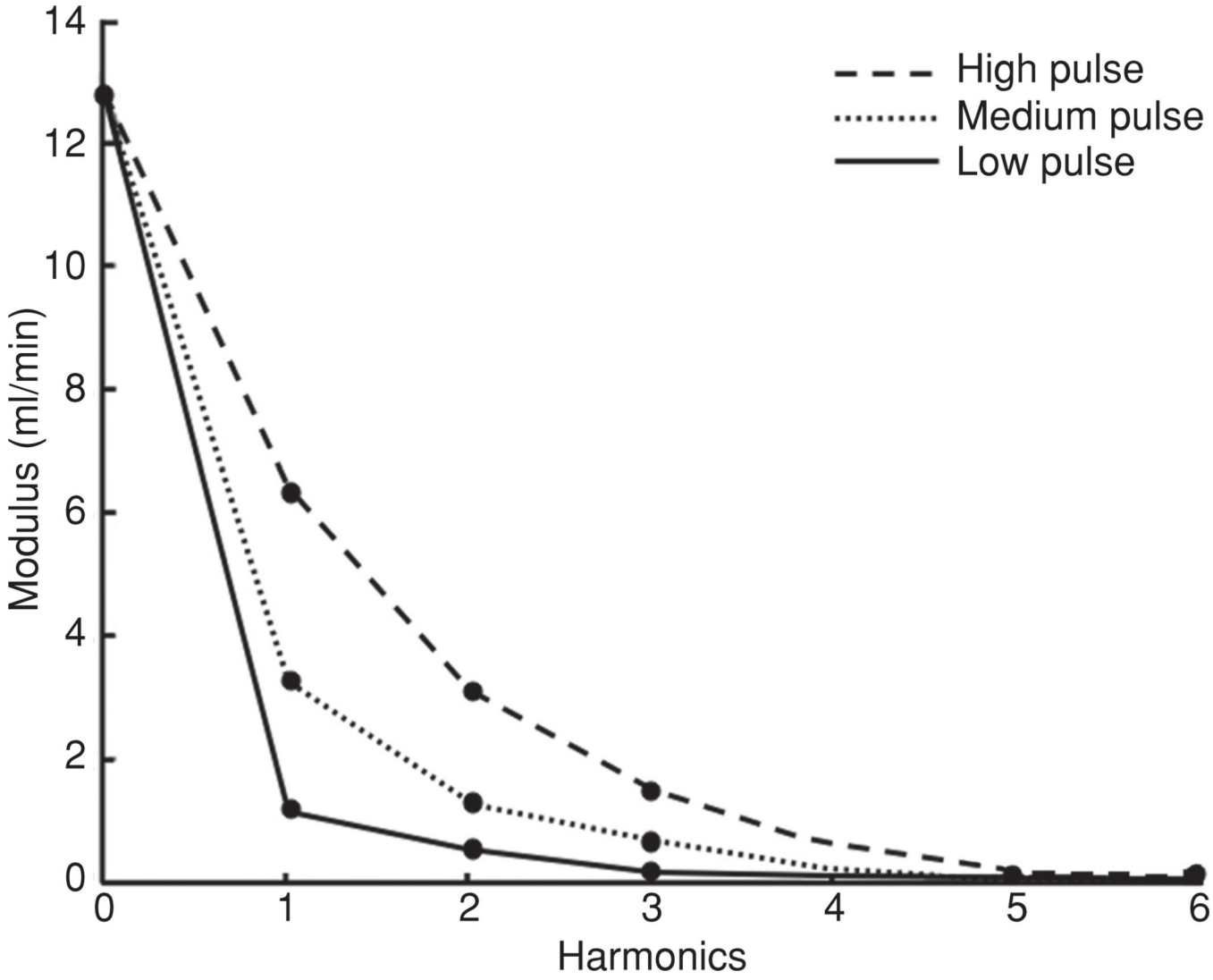

Figure 16.
Stiff arteries may extend high flow pulsatility into the pulmonary microcirculation, whereas in a normal compliant artery the capillaries experience semisteady flow.

Table 1

Average Power, Resting Conditions, Right Ventricle (mW) (87, 88)

Component	Dog (wt. 18.7 kg)	Man (wt. 76 kg)
Cardiac output, ml/s	42	82
Potential		
Steady	106.7	155
Oscillatory	3.5	73
Combined	146.2	228
Kinetic		
Steady	1.1	0.8
Oscillatory	9.9	14.1
Combined	11	14.9
Total		
Steady	107.8	155.8
Oscillatory	49.4	87.1
Combined	157.2	242.9
Oscillatory/total	31%	36%
Kinetic/total	7%	6%

Table 2

Boundary Conditions, Relative Effects of Resistance and Compliance on Pressure and Flow and Pros/Cons for Isolated Supported Ventricular Models: Pressure-Controlled (PCISV), End Systolic/Diastolic Volume-Controlled (VCISV), and Windkessel-Controlled (WCISV)

			Effect on pulse pressure and flow			
	Boundary condition	**Figure**	**Resistance**	**Compliance**	**Pros**	**Cons**
PCISV	Constant left artial pressure with distal mechanical analog	Figure 10	Low moderate	High	Mechanical analog of vasculature allows for direct control of hydraulic resistance and compliance	No direct control of end-systolic or end-diastolic conditions
VCISV	End-systolic/end-diastolic ventricular volume	Figure 11	High	Low	Direct control of end-systolic and end-diastolic conditions	No functioning atria, ventricular valves or distal hydraulic boundary conditions, assumes constant contractility
WCISV	Windkessel electrical analog (ventricular flows based on pressure input)	Figure 12	High	Low	Direct control of end-systolic and end-diastolic conditions with modeled hydraulic boundary condition	Distal hydraulic boundary conditions dependent on Windkessel function may not be physiologically accurate

Table 3

Effect of Changes in Resistance and Aortic Compliance on Aortic and Left Ventricular Pressure and Aortic Flow in Six Feline PCISV Hearts

	Increase in resistance (208% ± 13) without change in compliance (%)	Decrease in compliance (21% ± 4} without change in resistance (%)
P_{ao}		
P_S	124 ± 4	115 ± 4
P_D	138 ±7	52 ± 9
P_{mean}	133 ±6	78 ± 3
P_{LV}		
P_S	124 ± 4	113 ± 3
P_{mean}	130 ± 7	116 ± 7
Q_{ao}		
Q_p	74 ±2	66 ± 9
SV	66 ±3	79 ± 5
Q_{mean}	66 ±3	79 ± 5

NOTE: All results are given as percent changes ± standard error mean compared to the control situation.

P_{ao}, aortic pressure; P_S, systolic pressure; P_D, diastolic pressure; P_{mean}, mean pressure; P_{LV}, left ventricular pressure; Q_{ao}, aortic flow; SV, stroke volume; Q_{mean} mean flow (33).